A FEASIBILITY STUDY OF A THIN FILM OXYGEN PARTIAL PRESSURE SENSOR

Prepared for

National Aeronautics and Space Administration
Flight Instrument Division
Langley Research Center
Hampton, Virginia

Final Report

on

Contract No. NAS1-4617
RTI Project No. EU-200

December 8, 1964 to January 7, 1966

Submitted by:
J. J. Wortman

FOREWORD

This report was prepared by the Research Triangle Institute, Durham, North Carolina, on NASA Contract NAS1-4617, "Feasibility Study of a Thin Film Oxygen Partial Pressure Sensor". This work was administered under the direction of the Flight Instrument Division at Langley Research Center. Mr. William F. Leonard was project engineer for NASA.

This investigation began in December 1964 and was concluded in January 1966. It was performed by the Solid State Laboratory of the Research Triangle Institute under the general direction of Dr. R. M. Burger. Dr. J. J. Wortman was project leader. Mr. K. S. Canady and Mr. W. M. Aycock were active participants in the work.

CONTENTS

CONTENTS (continued)

LIST OF ILLUSTRATIONS

LIST OF ILLUSTRATIONS (continued)

LIST OF ILLUSTRATIONS (continued)

1. INTRODUCTION

The objective of this research has been to determine the feasibility of utilizing thin film devices as oxygen partial pressure sensors in the 0 to 300 mm Hg pressure range. A second objective has been to determine the advantages and disadvantages of thin film sensors with respect to conventional designs.

Three thin film techniques have been studied: (1) galvano-diffusion effect, (2) conductance modulation, and (3) controlled oxidation. The galvano-diffusion effect occurs in certain metal-dielectric-metal structures as a result of ionic diffusion in the dielectric. An electrical potential is generated between the metal electrodes which is a function of the oxygen pressure to which the device is exposed. This phenomenon has been studied in configurations utilizing a variety of metals and dielectric materials.

The conductance modulation techniques for utilizing thin films as oxygen partial pressure sensors is based on the fact that the conductance of certain thin films is a function of the oxygen partial pressure to which the films are exposed. Both adsorption of oxygen onto the surface and diffusion into the film can influence the electrical properties of the film material. Thin films of gold, hafnium, zirconium, titanium, and nickel have been studied with respect to their usefulness as oxygen partial pressure sensors.

The third thin film technique which has been studied is that of oxygen pressure dependent oxidation of films. This technique utilizes the insulation properties of metal oxides as well as the pressure dependent oxidation rate. Here the electrical resistance of the film is

changed by a physical reduction in the thickness of the conducting metal film.

Of the three techniques studied, the conductance modulation method utilizing gold as the film material has been found to be the most promising technique.

2. GALVANO-DIFFUSION EFFECT

The generation of a voltage in a metal-dielectric-metal structure, which is limited by a diffusion mechanism, will be called the galvano-diffusion effect.

It has been found experimentally that thin film metal-dielectric-metal sandwiches behave similar to galvanic cells if the proper material combinations are used and the device is operated at an elevated temperature in an oxidizing environment. The open circuit voltage produced between the two metal electrodes and the short-circuit current are each functions of the oxygen partial pressure to which the devices are exposed. The mechanism involves both a chemical reaction and a diffusion process, and requires an oxidizing metal and a nonoxidizing metal separated by a dielectric. The phenomenon has been studied both theoretically and experimentally. A theoretical model has been developed which is in qualitative agreement with experimental results.

2.1 Discussion

Galvano-diffusion is a phenomenon which occurs as the result of ionic diffusion through a thin insulating film and results in a self-generated electrical potential. In principle the phenomenon is simple and easy to understand. Consider an insultaing film which has the properties of being a poor electron conductor while simultaneously being a good ionic conductor (conductor of oxygen ions for example). If the two sides of the film have different ion concentrations, ions will diffuse through the film. Since the film is a poor electron

conductor, a charge will accumulate on the surfaces of the film as a result of the ionic diffusion.

In the absence of any means for the flow of electrons to neutralize the ionic charge between the two sides of the film, an electric field will be set up across the film opposing the ionic current. After a long time, the field will build up to the point where no ionic current will flow. If, however, an electrical conductor is attached to the two sides of the film or if the film is leaky, an electron current will flow through the conductor to compensate for the ionic current. In the case where there is no electron leakage through the insulator film, the external electron current in steady state will exactly equal the ionic current.

The above processes can occur naturally in the oxidation of metals when the metal oxide is an insulator. This is particularly true in metals that form protective oxides in oxidizing environments. Aluminum is a common example. In this case the oxidation occurring at the metal-insulator interface removes oxygen ions and thereby creates an oxygen ion concentration gradient across the film. As the oxide film increases in thickness the electron conduction is reduced which allows a field to be generated finally stopping the process.

The galvano-diffusion process can be formulated analytically by considering Poisson's equation, the continuity conditions, and the usual macroscopic diffusion equation for the ionic diffusion. This results in a system of nonlinear coupled partial differential equations. To formulate the equations for the general case with a time dependent thickness, consider a thin dielectric of thickness L(t). Let x be

the direction perpendicular to the plane of the film. The system of equations to be solved are:

$$J_i = -\mu\, C(x,t)E - D\frac{\partial C(x,t)}{\partial x} \tag{1}$$

$$\frac{\partial J_i}{\partial x} + \frac{\partial C(x,t)}{\partial t} = 0 \tag{2}$$

$$E(x,t) = \left(\frac{1}{\epsilon}\right)\int_o^x qC(x,t)dx + \frac{1}{\epsilon}\, q\sigma(0,t) \tag{3}$$

$$\sigma(0,t) = \sigma(0,0) - \int_o^t J_i(0,t)dt \tag{4}$$

$$\sigma(0,t) + \sigma(L(t),t) + \int_o^{L(t)} C(x,t)dx = 0 \tag{5}$$

J_i = ionic particle current density (number/sec·cm^2)

μ = mobility of the ions

D = diffusion coefficient

E = electric field at any point in the film

t = time

q = charge per ion

ϵ = dielectric constant of film

$\sigma(0,t)$ = surface density of the ions at x = 0 (number/cm^2)

$\sigma(L(t),t)$ = surface density of ions at x = L(t)

The initial and boundary conditions which are required are $\sigma(0,0)$, $C(0,0)$ and $C(L(0),0)$. Fromhold [1] has solved this problem for the steady state (neglecting transient conditions) homogeneous field case. This result for the ionic partial current is

$$J_i(t) = -\mu E\left[\frac{C(L(t),t) - C(0,t)\,\exp(-E\mu L(t)/D)}{1 - \exp(-E\mu L(t)/D)}\right] \tag{6}$$

This solution neglects any space charge effects due to the ionic charge in the insulator. Although the above solution was derived specifically for describing the oxidation of metals, it can be used to describe the galvano-diffusion effect.

For the present purposes it will be assumed that the ionic concentration is independent of time. As previously mentioned, there are two important limiting cases; (1) $E = 0$ and (2) $J_i = 0$. Actually both of these cases can be solved very simply from Eq. (1) without taking the limits in Eq. (6). Consider case (1) first. If $\frac{\mu EL(t)}{D} \ll 1$, then Eq. (6) reduces to

$$J_i = -D \frac{C(L(t)) - C(0)}{L(t)} \tag{7}$$

Note that $C(L(t))$ is independent of time although the film thickness L is a function of time. This low field condition can be arrived at physically by connecting a good electronic conductor to the two sides of the film ($E = 0$). When this is done the current in the external circuit is exactly equal to the ionic current. Denoting the current with zero field as the short-circuit current I_{sc}, it becomes

$$I_{sc} = qAD \frac{C(L(t)) - C(0)}{L(t)} \tag{8}$$

where A is the area of the film.

The temperature dependence of I_{sc} is the same as the temperature dependence of the diffusion coefficient. Typically D is related to temperature as follows

$$D = D_o e^{-E_a/kT}, \tag{9}$$

where D_o is a constant and E_a is the activation energy. Using this relationship, I_{sc} becomes

$$I_{sc} = qAD_o \, e^{-E_a/kT} \, \frac{C(L(t)) - C(0)}{L(t)} \qquad (10)$$

In the second case where $J_{\pm} = 0$, Eq. (6) reduces to

$$E = \frac{kT}{eL(t)} \ln \frac{C(0)}{C(L(t))} , \qquad (11)$$

or

$$V_{OC} = E\,L(t) = \frac{kT}{e} \ln \frac{C(0)}{C(L(t))} , \qquad (12)$$

where V_{OC} is the open-circuit voltage. This shows that the voltage across the film is directly proportional to temperature. Further the external voltage is independent of film thickness.

The open circuit case is very difficult if not impossible to obtain experimentally since most ionic conductors are to some extent electron conductors. If there is any electron leakage, V_{OC} will never be realized physically. Shown in Fig. 1 is an equivalent circuit for the film. It is proposed that the film can be represented by four parallel elements (current generator, leakage resistor, diode, and capacitor) in series with a resistor. The current generator is the ionic current. The leakage resistor is the electronic resistance offered by the sample, the diode is shown to account for nonsymmetric electronic barriers that could occur and the capacitance is obvious. The series resistance could result from such things as contact resistance. In the ideal case only G and C appear with $R_s = 0$ and

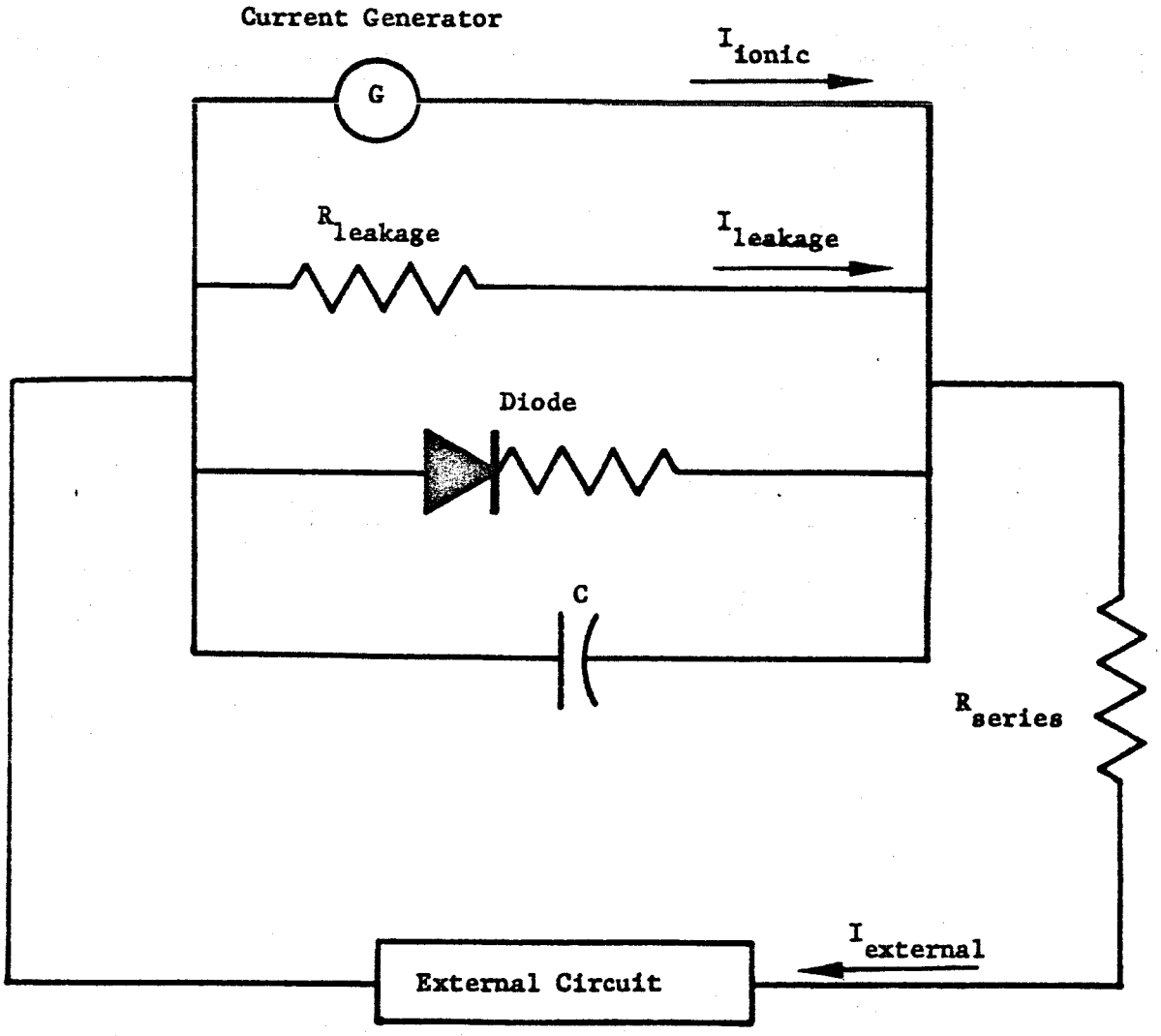

Fig. 1. Proposed Equivalent Circuit for the Dielectric Film

$R_{leakage} = \infty$. Neglecting the diode and capacitor, the open-circuit voltage from the equivalent circuit and Eq. (6) is

$$V_{OC} = \frac{kT}{e} \ell n \frac{C(0) + L(t)/q\mu A R_{leakage}}{C(L(t)) + L(t)/q\mu A R_{leakage}} . \qquad (13)$$

It can be seen from Eq. (13) that the leakage resistance reduces the open-circuit voltage. In the limit as $R_{leakage}$ approaches zero V_{OC} approaches zero as expected.

Consider the practical case where the insulator is a thin layer of metal oxide grown on the parent metal such as aluminum oxide (Al_2O_3) grown on aluminum. If the dielectric thickness is small, then the oxide will continue to grow if the sample is exposed to an oxygen environment. Here the ions are oxygen. Assume for the present that C(0) and C(L(t)) are constant and fixed by the environment and oxidation process respectively. In the short-circuit case, the external current is given by Eq. (8). Ions that diffuse through the oxide cause an increase in the oxide thickness by oxidizing the metal. The thickness is related to ion current by

$$\frac{dL(t)}{dt} = R J_i(t) , \qquad (14)$$

where R is the volume of oxide formed per electron that flows in the external circuit. Solving Eqs. (8) and (14) for the short-circuit gives

$$I_{sc} = \frac{I(0)}{\sqrt{1 + \frac{2RI(0)}{L(0)A} t}} , \qquad (15)$$

where I(0) and L(0) are the current and thickness at t = 0. From Eqs. (14) and (15) it is seen that

$$\frac{dL(t)}{dt} = \frac{I(0)L(0)R}{AL(t)} = \frac{k}{L(t)} , \tag{16}$$

where k is a rate constant independent of time and thickness. This means the oxide growth is parabolic which is common in the oxidation of many materials. The time dependent thickness is then, from Eq. (16)

$$L(t) = L(0)\sqrt{1 + \frac{2RI(0)}{L(0)A}\, t} . \tag{17}$$

The preceding treatment of the galvano-diffusion effect has been based on the assumption that no space charge effects are important. In practice this may be a poor assumption. If such effects are important the solution is difficult to obtain. Fromhold has treated some of the oxidation problems when space charge effects are important [2]. Also transient effects fall into much the same category as space charge effects in trying to describe the effect.

The galvano-diffusion effect can be utilized as an oxygen partial pressure sensor. A cross section of the thin film system used for this purpose is shown in Fig. 2. The structure is a metal-dielectric-metal oxide-metal sandwich. The purpose of the nonoxidizing metal, M′, between the environment and the dielectric is twofold; (1) to provide for electrical contact and (2) to act as a supplier of oxygen. The purpose of the oxidizable metal, M, is to provide a sink for the oxygen ions that diffuse through the dielectric and thereby maintain an ionic concentration gradient across the dielectric.

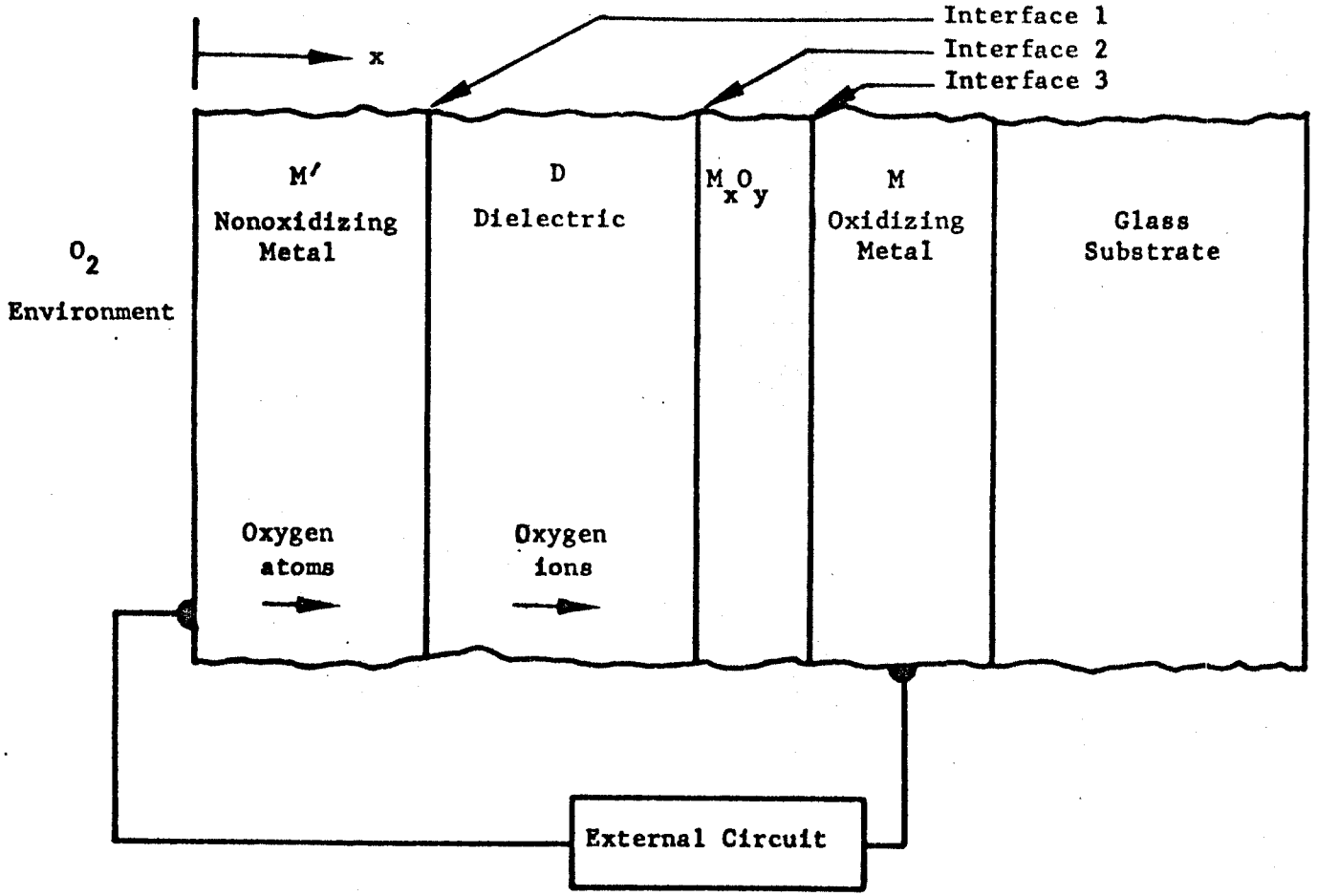

Fig. 2. Cross Section of a Thin Film Oxygen Partial Pressure Sensor

A metal oxide layer M_xO_y is shown between the dielectric and metal M. This metal oxide may or may not be the same material as the dielectric. For example, the dielectric could be oxidized aluminum and the metal oxide in this case could also be oxidized aluminum. In other cases the dielectric might be evaporated silicon monoxide and the metal oxide might be aluminum oxide (an insulator) or manganese oxide (a conductor).

The electronic current which the sensor is capable of delivering to an external circuit is limited by several mechanisms:

1. The rate at which oxygen is adsorbed onto the surface of the nonoxidizing metal electrode.
2. The rate at which oxygen diffuses through the nonoxidizing electrode.
3. The rate at which oxygen ions are produced at interface 1.
4. The rate at which oxygen ions diffuse through the insulator.
5. The rate of oxidation at the oxidizable electrode.

In order for the sensor to be sensitive to oxygen partial pressure, at least one of the above processes must be a function of the environmental oxygen partial pressure.

Consider the first of the above processes. There have been many theories proposed for the adsorption of gas atoms and molecules on the surface of materials [3]. Without considering particular materials and particular gases, it is practically impossible to describe in detail the adsorption. The most common theory for monolayer absorption is that of Langmiur [4]. This theory relates the volume adsorbed, V, to the absolute pressure of the gas, P, as follows:

$$V = \frac{V_s bP}{1 + bP} \tag{18}$$

where b and V_s are constants depending on the material and temperature.

The Brunauer-Emmett-Teller theory (BET) [5] is the most commonly used theory of multilayer adsorption. The equation for a free surface is

$$V = \frac{V_s cx}{1 - x} \cdot \frac{1 - (n + 1)x^n + nx^{n+1}}{1 + (c - 1)x - cx^{n+1}}, \tag{19}$$

where $x = P/P_o$ and c, V_s, P are constants at any given temperature. Here n is the number of layers. If n = 1, Eq. (19) reduces to that of Eq. (18) for monolayer adsorption. Both the Langmiur and BET equations have been derived from statistical considerations. Consequently they give little information on the physics of the interactions of the gas atoms with the surface and the adsorber sites.

The second limiting factor is the diffusion of oxygen through the nonoxidizing electrode. Since this diffusion probably takes place as atomic or molecular diffusion (nonionic), Eq. (1) can be used with E = 0, i.e.,

$$J_{ox} = -D_{ox} \frac{\partial C_{ox}}{\partial x} \tag{20}$$

where the subscript ox denotes oxygen atoms. Assuming a linear concentration gradient gives

$$J_{ox} = -D_{ox} \frac{(C_{ox}(0) - C_{ox}(L_{M'}))}{L_{M'}} \tag{21}$$

where $L_{M'}$ is the thickness of M′. The above assumption is expected to be reasonable since M′ in general will be a very thin layer. $C_0(0)$ is equal to V in Eqs. (18) and (19).

The concentration of oxygen ions at interface 1 (item 3) is expected to be proportional to the concentration of oxygen atoms at the interface. The rate of supply of ions would be limited by the concentration of atoms.

Item (4) is the galvano-diffusion which has already been discussed. If the metal oxide is an insulator, the same theory holds as that for the dielectric. If the oxide is a conductor the process is the same as for the nonoxidizing electrode. Item (5), the chemical reaction rate is assumed to not limit the other processes.

The above discussion should not be taken as a complete treatment of the indicated processes. It is intended that the information provide some insight into the magnitude of the problem. To continue the discussion of the individual processes further would require a much detailed study of particular materials and their combinations. Much of the information required for a detailed treatment is not available and is not within the limits of this work.

From the limited discussions given it is, however, possible to reach some qualitative conclusions. By combining the several processes, it can be seen that the external short-circuit current of the practical system is a function of the oxygen partial pressure. This is obtained by successively solving for the concentrations at each interface in the system.

The experimental discussion which follows considers a variety of materials which have been studied using the system presented above.

2.2 Experimental Techniques

Two different types of experimental test stations were constructed; the primary purpose of which was to control the temperature and environment of the test samples. Temperature could be controlled from room temperature to 1000°C and environments could be changed from air to argon, oxygen, helium, nitrogen, or carbon dioxide or any percentages of these.

Figure 3 shows a Hevi-Duty type 70-T tube oven, a Barber Colman model 293 temperature controller, and a Fischer and Porter flow meter. Inside the tube oven was a 24 inch length of pyrex glass tube covered by brass tubing, for electrical ground and heat distribution. A chromel-alumel thermocouple was placed next to the heater coils of the oven and connected to the temperature controller; temperature control was $\pm$ 1°C. The various gases were supplied from compressed gas bottles. The gas flow rate was controlled by gas regulator and needle valves. Fischer and Porter flow meters were used to monitor flow rate from the bottles to and through the pyrex tube in the oven. Ordinarily, total gas flow rate ranged from 100 to 300 cc/min. The total gas pressure was one atmosphere since the flow was low and one end of the tube was open to the atmosphere.

Figure 4 shows an environmental chamber. Heat is supplied to the chamber by Watlow Firerod heaters, and temperature was controlled by a chromel-alumel thermocouple connected to a Barber-Coleman model 293 temperature controller. A small bell jar was placed over the base plate and clamped down. Needle-valves controlled the entry and exit of gases

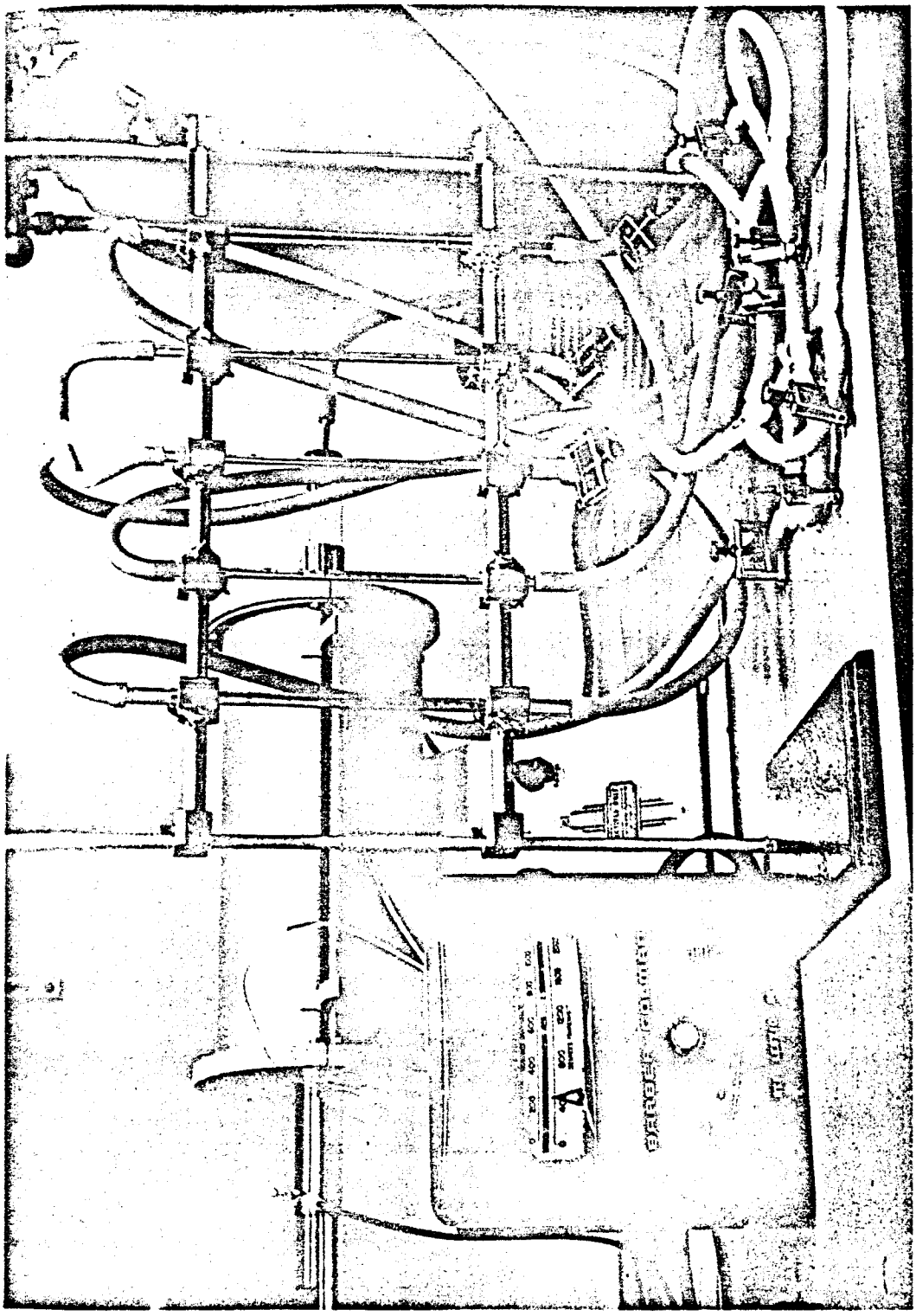

Fig. 3. Photograph of Tube Oven Experimental Chamber

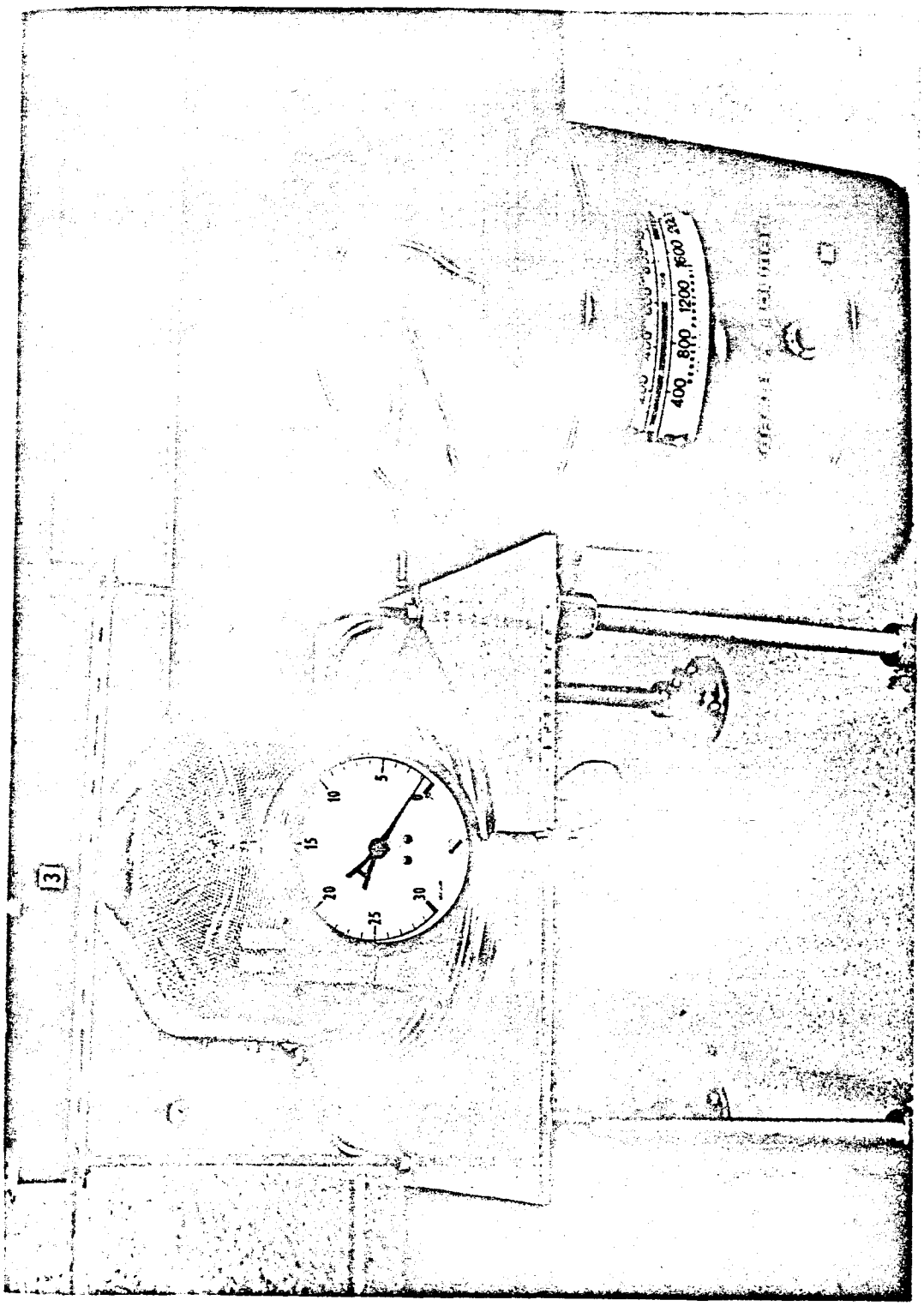

Fig. 4. Photograph of Vacuum Experimental Chamber

within the chamber. The chamber provided for either pressure measurements (greater than one atmosphere) or vacuum partial pressure measurements.

In order to fabricate the galvano-diffusion structure, vacuum evaporation techniques were utilized. For the oxidizing metal electrode, various metals were evaporated such as aluminum, lead, copper, silver, manganese, and bismuth; standard techniques were used for evaporation [6]. For the dielectrics, an R. D. Mathis oven was used for the evaporation of silicon monoxide and a molybdenum boat was used for the evaporation of magnesium fluoride. For the top electrode gold, manganese, and silver were evaporated from tungsten filaments. Evaporations were made in the pressure range of 10^{-5} torr. In most cases the entire sample was fabricated without breaking vacuum. It was necessary to have ultra-clean substrates on which to evaporate. Two types of substrates were used: pyrex glass slides and single crystal silicon wafers. The following cleaning procedure was used to clean the substrates;

A. Pyrex Slides

1. Scrub slides with alconox solution.
2. Place slides in alconox solution in ultra-sonic vibrator for five minutes.
3. Rinse slides in distilled water.
4. Repeat step 2.
5. Rinse slides in distilled water and place in distilled water in ultra-sonic vibrator for five minutes.
6. Rinse slides in methyl alcohol.
7. Rinse slides in trichloroethylene.
8. Boil slides in trichloroethylene for five minutes.

9. Rinse in methyl alcohol.
10. Place slides in methyl alcohol in ultra-sonic vibrator for five minutes.
11. Rinse in methyl alcohol and store in methyl alcohol until used.

B. Silicon Wafers

1. Rinse wafers in distilled water.
2. Rinse in methyl alcohol.
3. Boil wafers in trichloroethylene for five minutes.
4. Boil wafers in nitric acid for five minutes.
5. Rinse in methyl alcohol.
6. Etch wafers in hydrofluoric acid for a few seconds.
7. Rinse in methyl alcohol.
8. Rinse in distilled water.
9. Rinse and store in methyl alcohol until used.

In each case the methyl alcohol from the final step is dried from the substrate by means of forced hot air heat immediately before placing in the vacuum system.

Good evaporations were made either by heating the substrate to 200°C or leaving the substrates unheated. The thicknesses of all evaporations were measured by an oscillating quartz crystal mass monitor.

Electrical contact was accomplished in the tube furnace chamber by placing the sample on a small steel block to which was attached gold wire probes. Ceramic tubes were used to feed the gold wire into the oven. A thermo-couple was imbedded in the steel block to measure its temperature; the sample substrate was in thermal contact with the steel block. See Figs. 5 and 6.

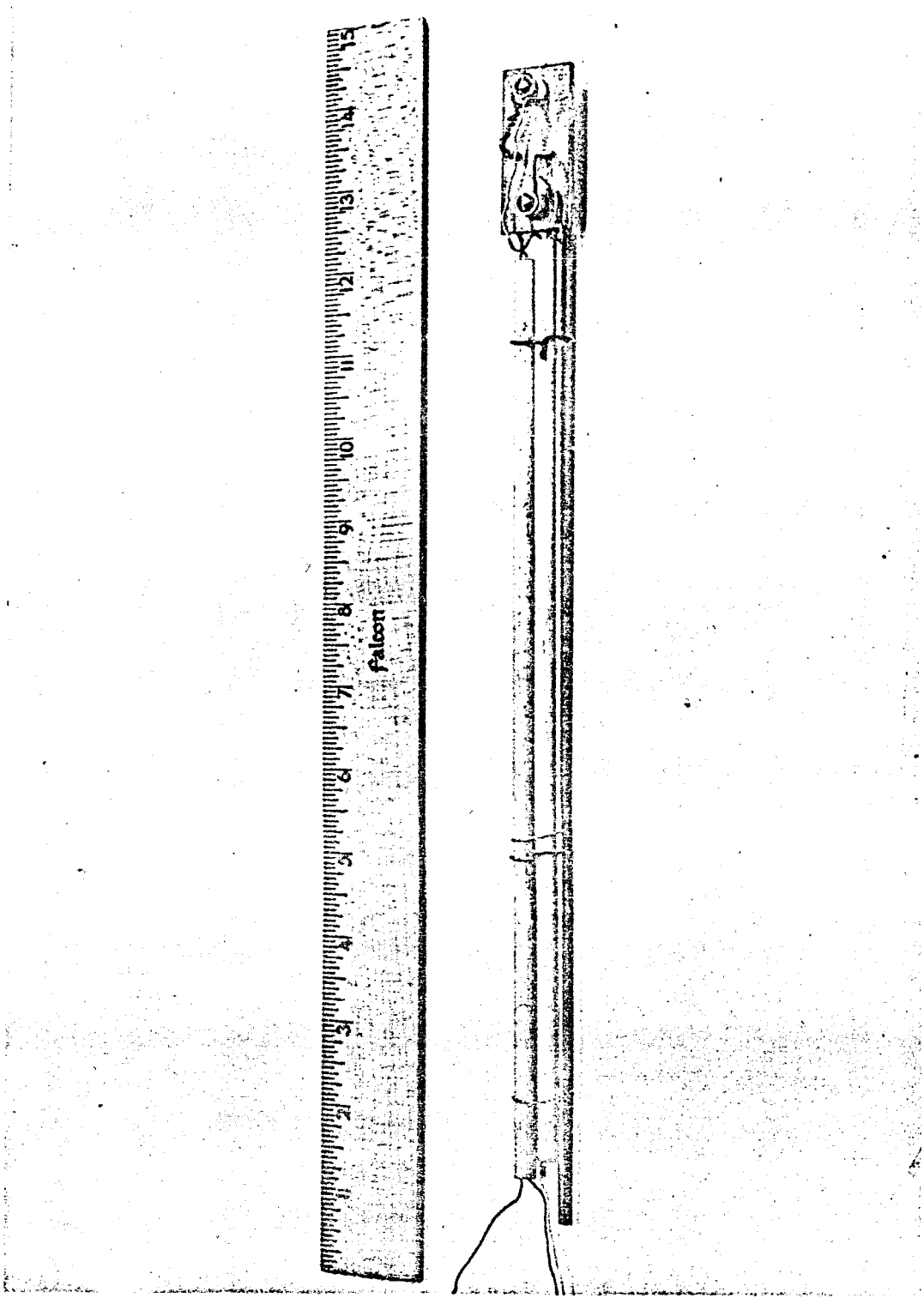

Fig. 5. Photograph of Sample Holder Used in Tube Oven

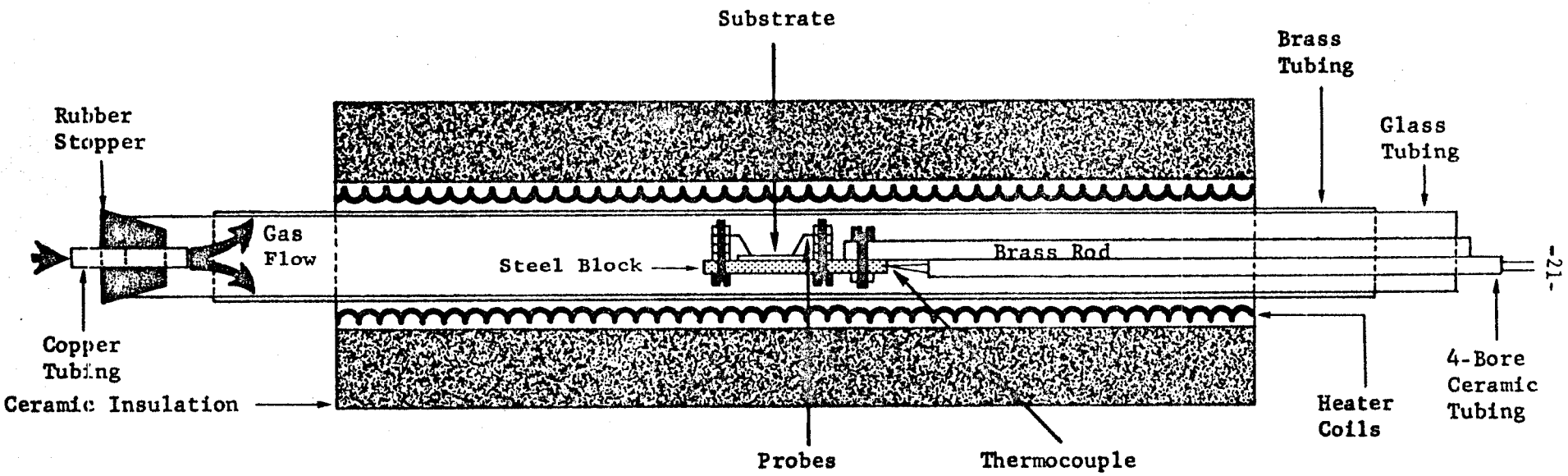

Fig. 6. Tube Oven Experimental Chamber (Cross Section View)

The short-circuit current produced by the samples was measured. The internal impedance of most samples was greater than fifty megohms. A Hewlett-Packard DC micro-volt-ammeter (hp 425 A) with an input impedance of one megohm was used to measure the short-circuit current output.

It is necessary in the galvano-diffusion samples to make electrical contact to both the nonoxidizing and the oxidizing electrodes. In general the structures were of the cross-stripe type shown in Fig. 7. The top electrode or nonoxidizing electrode is in general a good electrical conductor which allows one to easily make electrical contact. The oxidizing electrode falls in a different category however. Since it oxidizes in an oxygen environment, the parts not covered by the dielectric are immediately oxidized when tested. In cases where the metal oxide was an insulator it was necessary to evaporate a nonoxidizing electrode underneath the oxidizable electrode to make electrical contact. Some oxidizing electrodes such as aluminum form protective oxide layers that are thin. In these cases probes can be penetrated through the oxide to make contact to the underlying metal.

The samples have been classified according to the structure. For example, a glass-gold-bismuth-silicon monoxide-gold structure has a glass substrate, a gold base metal to make contact to the bismuth, a bismuth oxidizing electrode, a silicon monoxide dielectric, and a gold nonoxidizing electrode. For these structures, as all others tested, the top electrode (nonoxidizable) was found to be electrically positive, and the bottom (oxidizable) electrically negative. The results obtained on various structures are discussed in the following section.

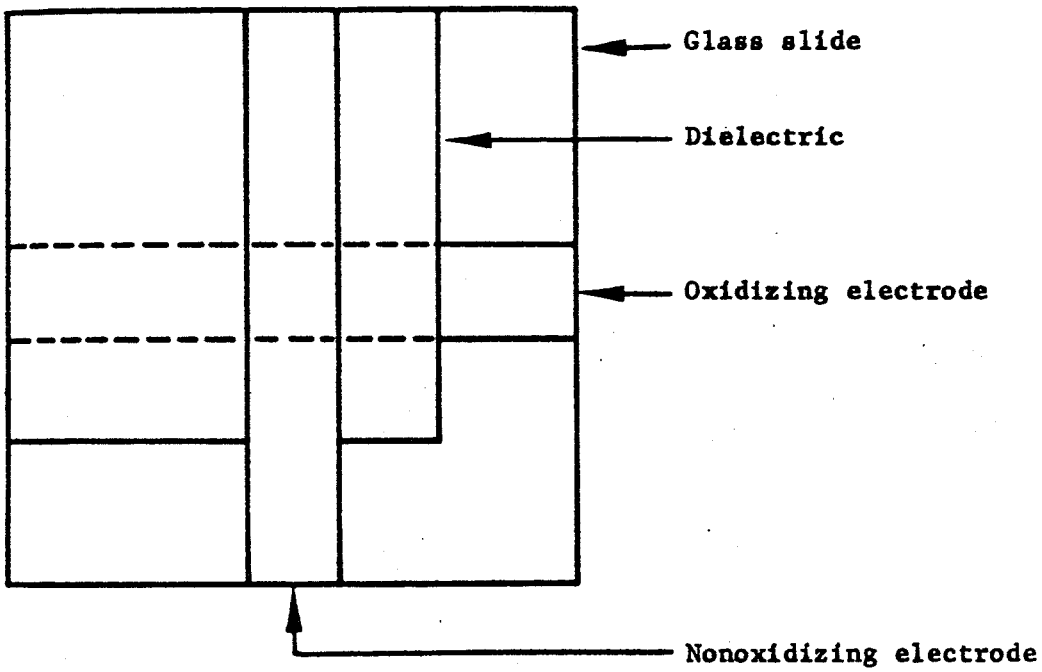

Fig. 7. Cross-Stripe Geometry of Oxygen Sensor

2.2.1 Glass-Aluminum-Aluminum Oxide-Gold

Samples of Al-Al_2O_3-Au were prepared by first evaporating a thin stripe of aluminum onto the glass substrates. Following this evaporation, the samples were removed from the vacuum chamber. A portion of the stripe was then submerged into an anodizing solution of 3% tartaric acid. The anodizing system gave approximately 13 Å of oxide per volt. After anodizing, the sample was again placed into the vacuum chamber and a gold stripe was evaporated perpendicular to the aluminum stripe. The active area was that defined by the area common to both the aluminum and gold. Typical thicknesses were 1500 Å of aluminum, 150 Å of aluminum oxide, and 1000 Å of gold. The active area was approximately 4 square mm.

These samples were tested initially in room air (containing normal amounts of water vapor). Figure 8 is a plot of the short-circuit current as a function of time for a typical sample. Comparison of this data with the analytical expression for I_{sc} (Eq. 15) shows that there is reasonable agreement after the sample has been in operation for several hours. In the early period of operation one would expect that holes and vacancies in the oxide would be filled along with an annealing of the oxide.

Figure 9 is a plot of self-generated voltage as a function of current delivered to the external circuit. Four different temperatures are shown. From the data it is seen that $V_{OC} = 2.5 \times 10^{-3}$ T volts/°C and $I_{sc} = 1.8 \times 10^{-8} \exp(-1.3/kT)$ amps. Each of these parameters has the predicted temperature dependence. Figure 10 is a plot of $\ell n\ I_{sc}$ as a function of 1/T. The two curves were obtained from similar samples. Each of the samples gave straight line plots and were displaced only in magnitude.

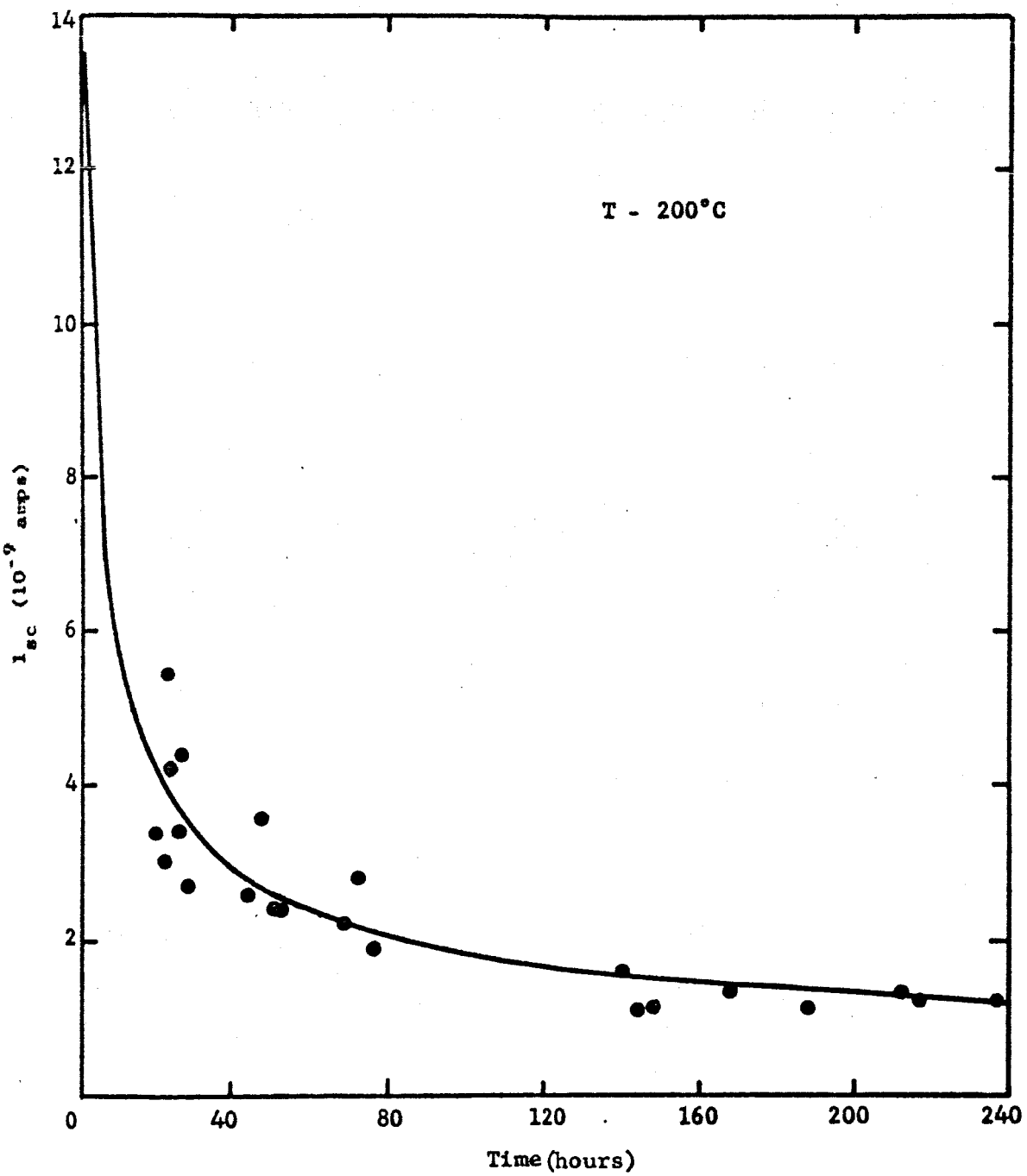

Fig. 8. Short-Circuit Current as a Function of Time

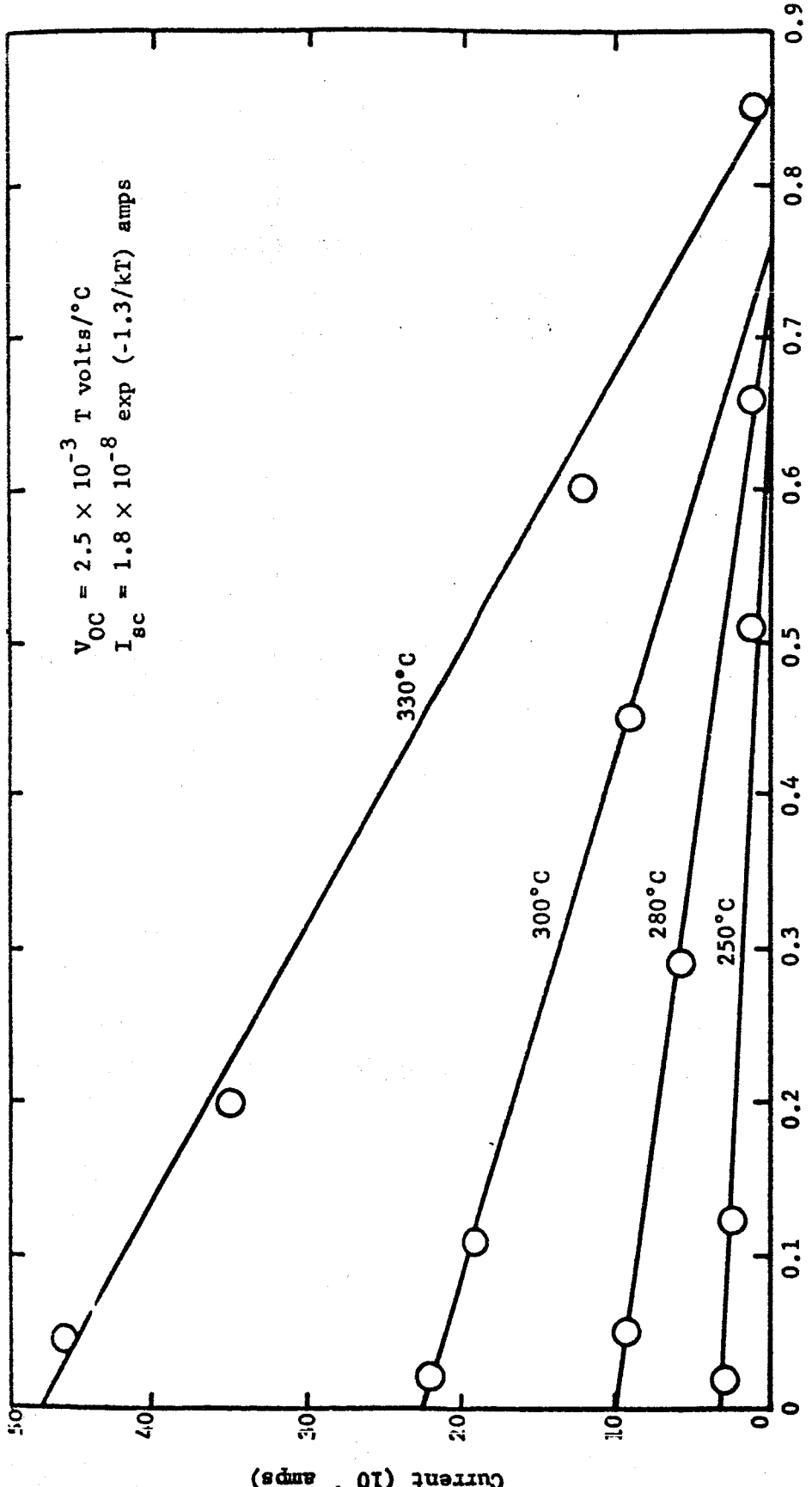

Fig. 9. V-I Plot at Several Operating Temperatures for a Typical Sample

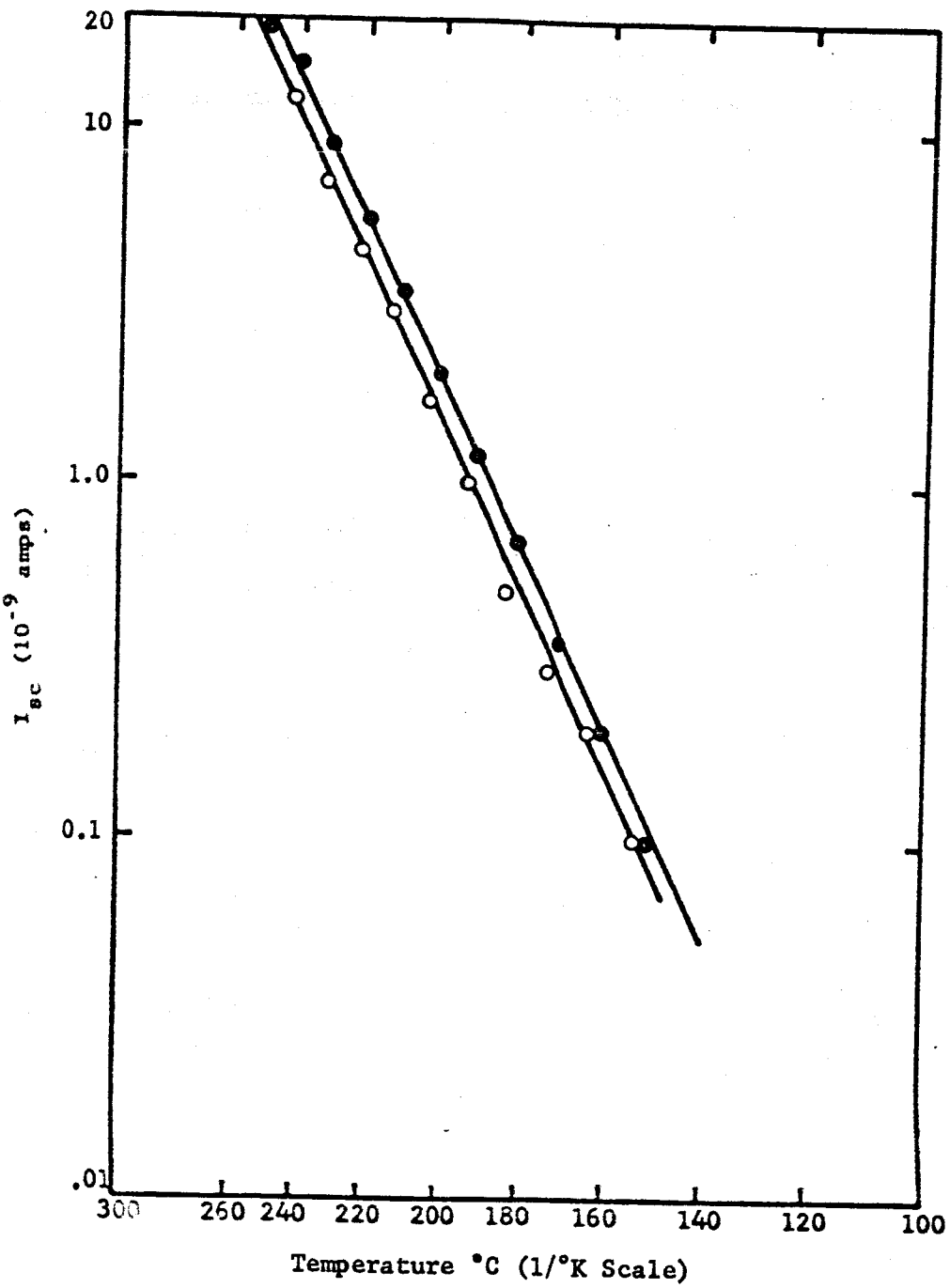

Fig. 10. Short-Circuit Current vs Reciprocal Temperature for Two Similar Samples

As already mentioned the above tests were performed in room air. It was found that the short-circuit current was extremely sensitive to moisture. Tests performed in controlled humidity environments of O_2, N_2 and Ar gave considerable variation in the results. Figure 11 is a typical plot of a cycling experiment. Note the large transients which occur when the gas is cycled.

It was concluded that due to the moisture sensitivity and to lack of control in oxide properties that a better dielectric material could be found for the present purposes.

2.2.2 Glass-Aluminum-Silicon Monoxide-Gold

These structures were made by evaporating a stripe of aluminum onto a glass slide, then evaporating a square of silicon monoxide atop the aluminum, and finally evaporating a stripe of gold on the silicon monoxide perpendicular to and insulated from the aluminum (see Fig. 7). The material thicknesses which were found to produce the best results were 1000 Å of aluminum, 500 Å of silicon monoxide, and 750 Å of gold.

These samples were tested in the tube furnace and found to exhibit short-circuit current outputs of about one nanoampere per square mm. The short-circuit current was found to depend on the environment and temperature.

Figure 12 shows the current output versus time for a typical sample for different gases and mixtures of gases. This data was taken with the sample at a temperature of 300°C. Figure 13 shows a sample with the same metal and dielectric thicknesses at 160°C. Upon comparison of Figs. 12 and 13, it is noted that at the lower temperature transient

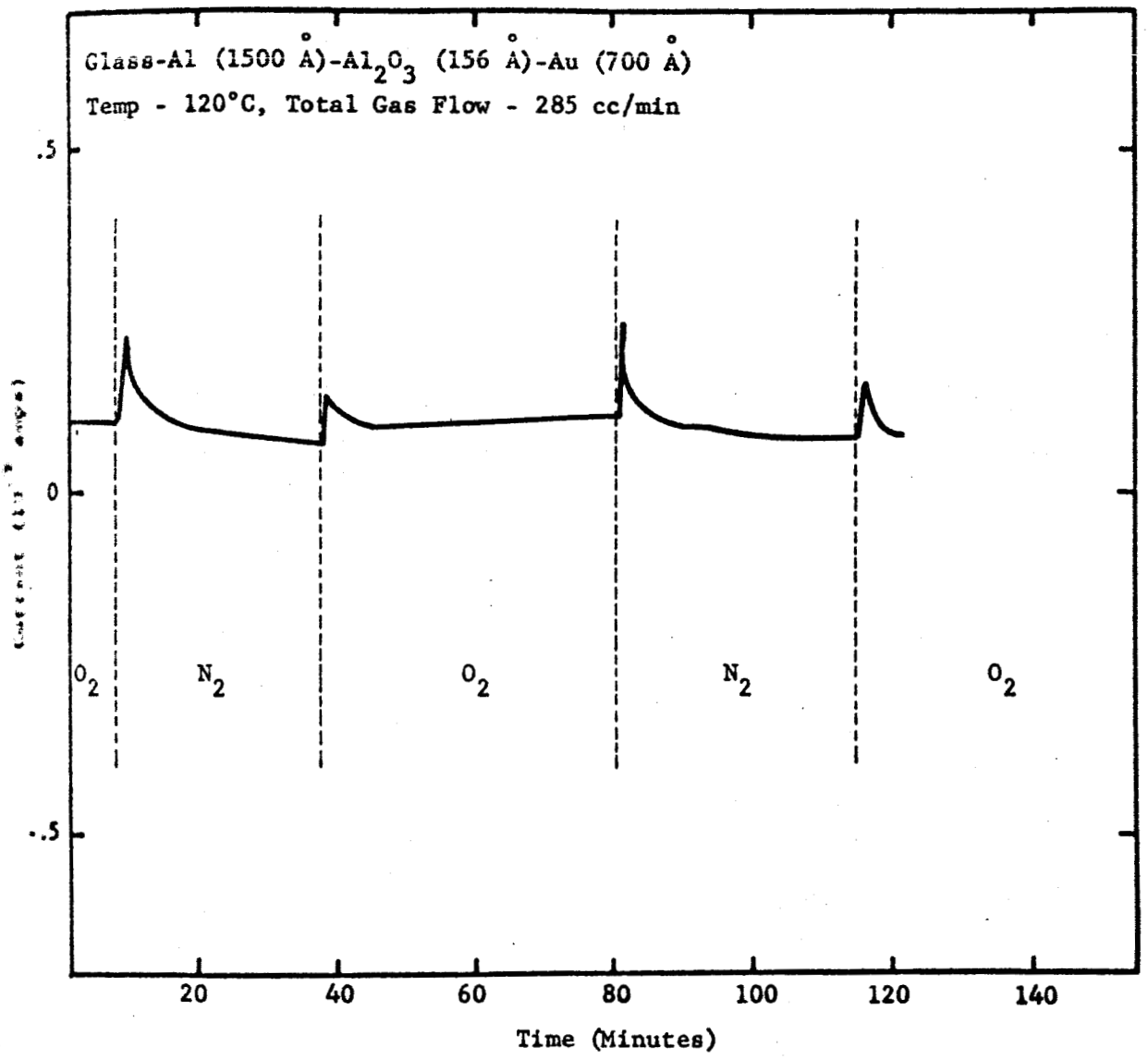

Fig. 11. Short-Circuit Current vs Time in Various Environments

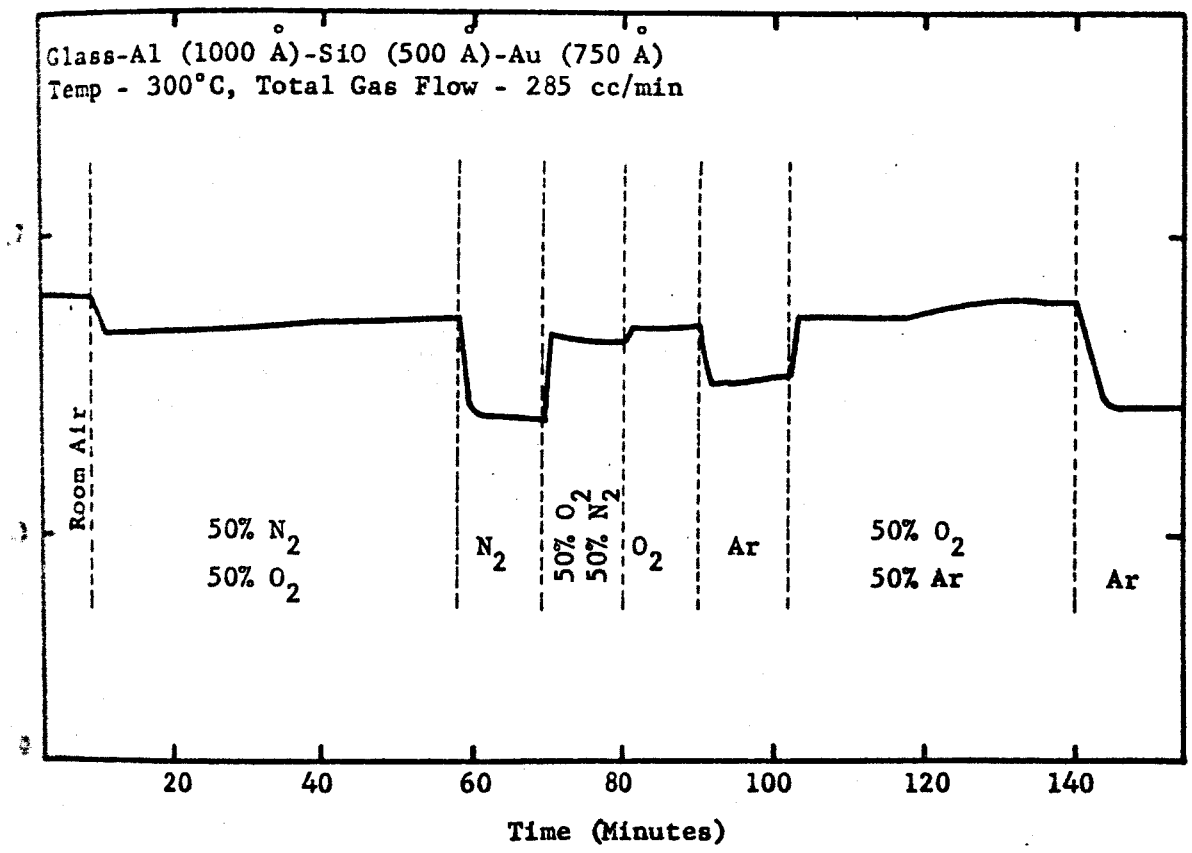

Fig. 12. Short-Circuit Current vs Time in Various Environments

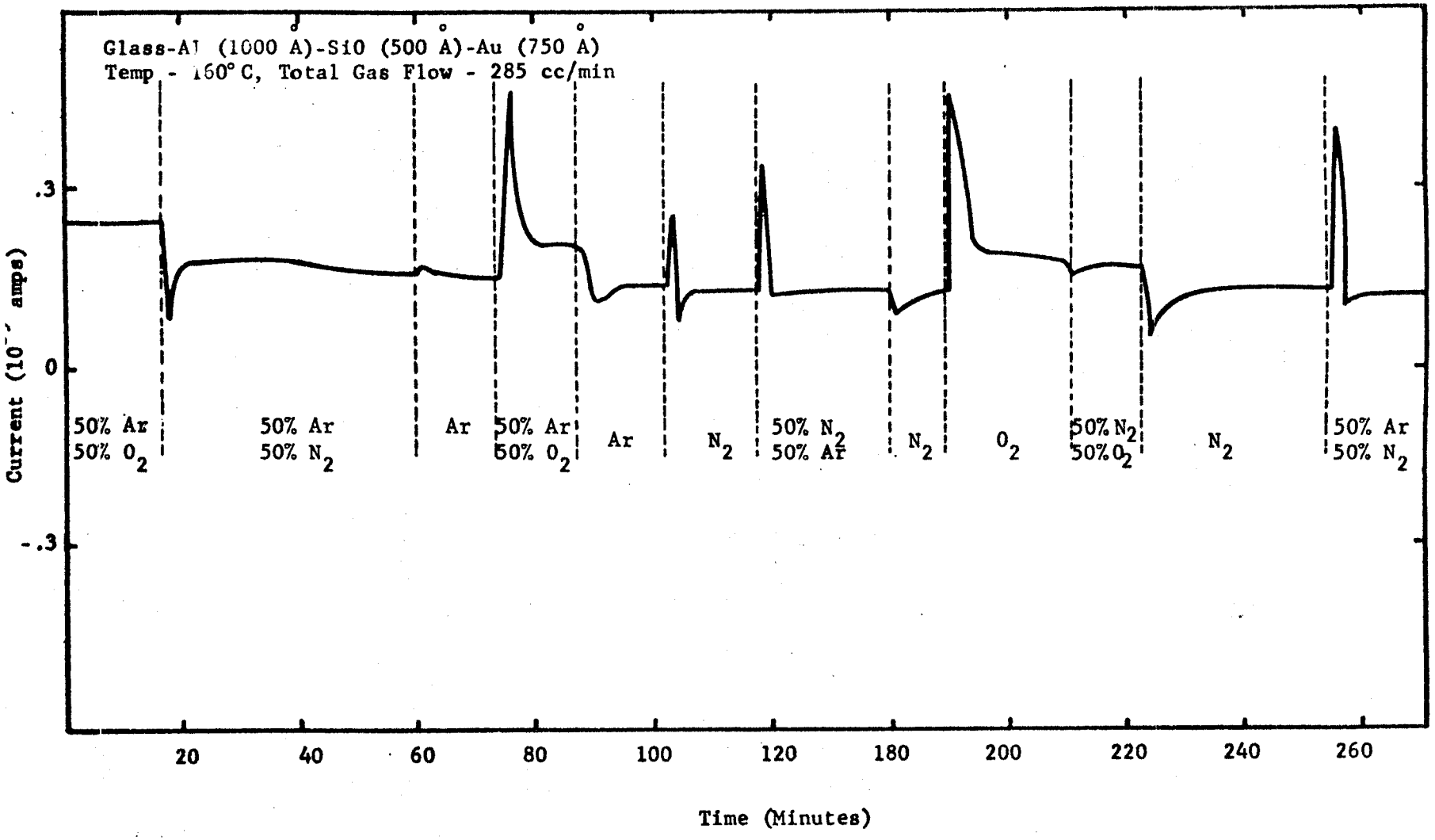

Fig. 13. Short-Circuit Current vs Time for Various Environments

effects are present when the environment changes, while at the high temperature transient effects are not present. These figures also show the time response of the current output due to a gas change. The rise times are on the order of one minute and the fall times are about four minutes. Comparison of these two graphs and other data on this type of sample led to the conclusion that the optimum range of temperature for maximum oxygen sensitivity is from 250°C to 300°C.

The various short-circuit current levels are dependent on the operating temperature and age of the sample. The age of the sample is defined as the time of actual use in circuitry at an elevated temperature. This age does not include shelf life. The data shown in Fig. 14 is from a sample with an age of 4 days, while Figs. 12 and 13 are for samples with ages of 18 days and one day respectively. The current level of the sample of Fig. 14 is high compared to the samples of Figs. 12 and 13 because of its high operating temperature (270°C compared to 160°C of Fig. 13) and its short age (4 days compared to 18 days of Fig. 12). The current level of the sample of Fig. 13 is low because of low temperature; the current level of the sample of Fig. 12 is low because of its long age.

2.2.3 Silicon-Aluminum-Magnesium Fluoride or Silicon Monoxide-Gold

On these structures two aluminum dots were evaporated on a silicon substrate which had been cleaned by the procedure previously described. Following the dot evaporation either MgF_2 or SiO was evaporated completely covering one of the aluminum dots. A gold dot was then evaporated on top of the dielectric. In this case, electrical contact was made to the uncovered aluminum dot through the silicon substrate to the bottom electrode (see Fig. 15).

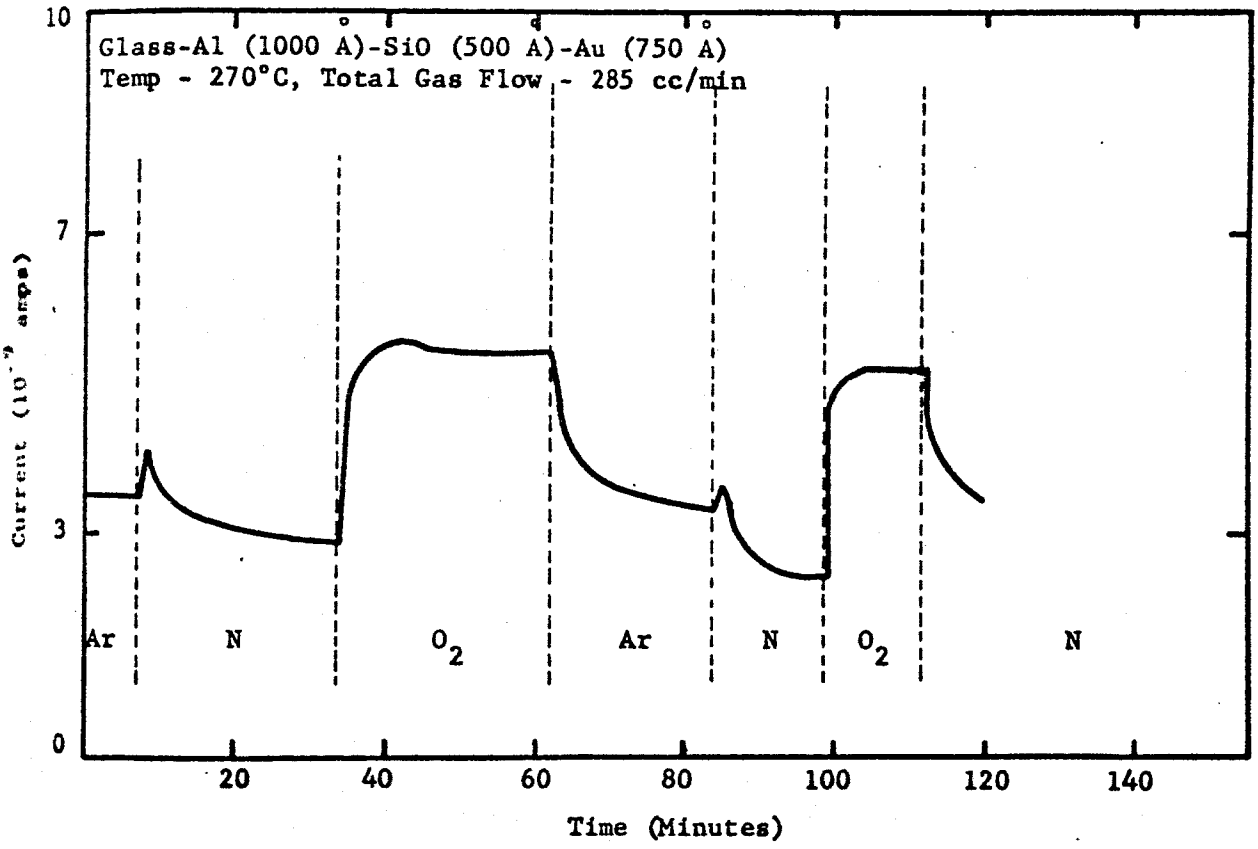

Fig. 14. Short-Circuit Current vs Time in Various Environments

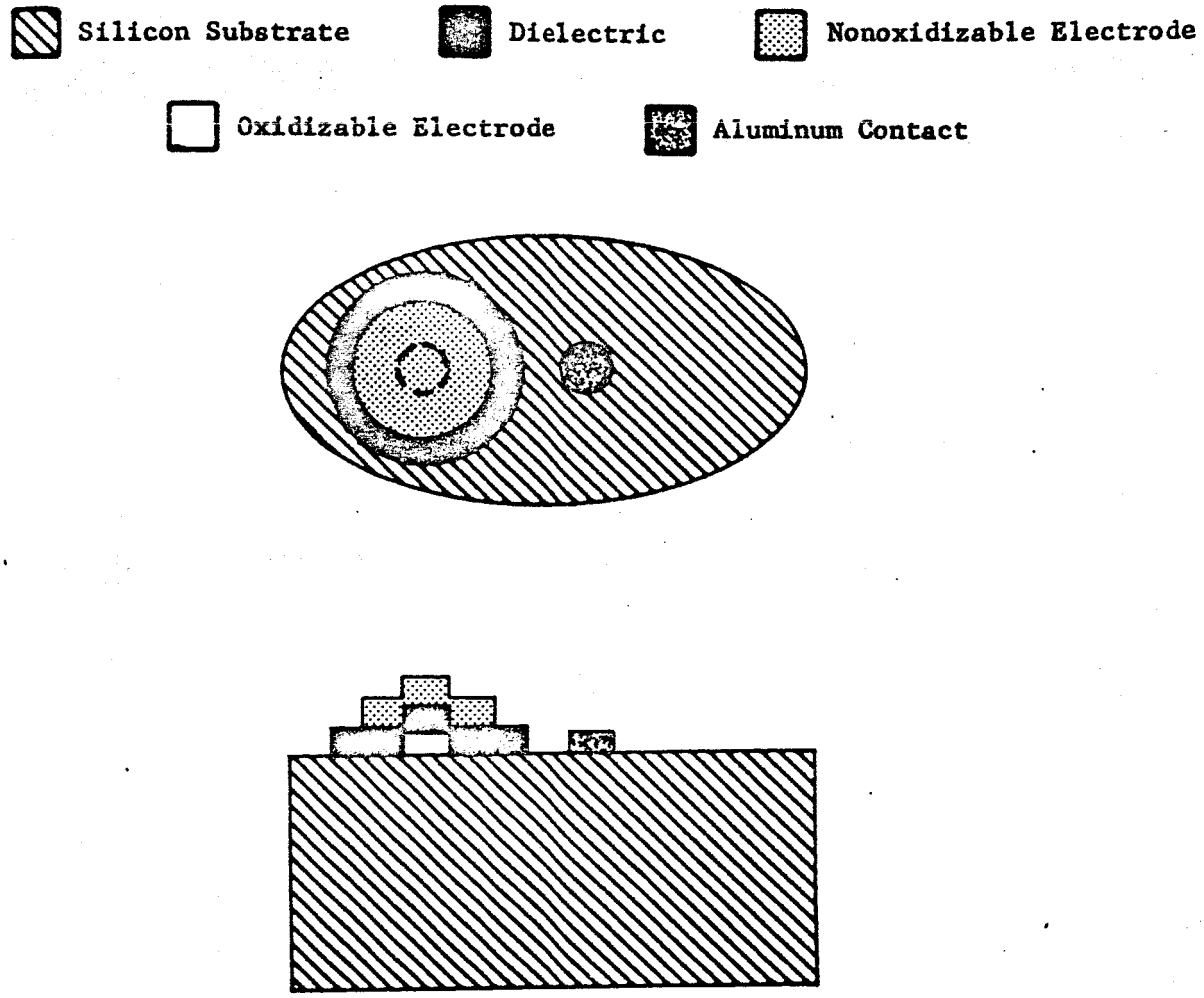

Fig. 15. Top and Cross Sectional View of Oxygen Sensor Evaporated on Silicon Substrate

Temperature and environmental tests were run on these samples in the tube furnace. As indicated by Fig. 16, these samples were very sensitive to water vapor. The largest current output was observed when the environment was room air containing water vapor.

Because of this extreme sensitivity to water vapor, even at elevated temperatures, this type of substrate and corresponding geometry was abandoned. Emphasis was then placed on using a glass substrate with a cross-stripe geometry and an evaporated dielectric.

2.2.4 Glass-Aluminum-Silicon Monoxide-Silver

Previous structures had been manufactured with gold, which is nonoxidizable, as the top electrode. Al-SiO-Ag structures were made in the geometry of Fig. 7 with 1000 Å of aluminum as the bottom electrode, 500 Å of silicon monoxide as the dielectric, and 875 Å of silver, an oxidizable metal, as the top electrode.

As in previous structures short-circuit transient responses were obtained at room temperature and at slightly higher temperatures by cycling the environments. However, steady-state responses to oxygen could be obtained only at elevated temperatures. In this case, the structure exhibited about 20 to 30 nanoamperes higher short-circuit current output in an oxygen atmosphere than in any other environment.

Figure 17 shows the transient response at room temperature. A similar response was also noted for the sample at 160°C. Figure 18 shows the current versus time plot for the same sample at 375°C. Notice that only at the high temperature of 375°C does this type of structure give a steady-state response in oxygen.

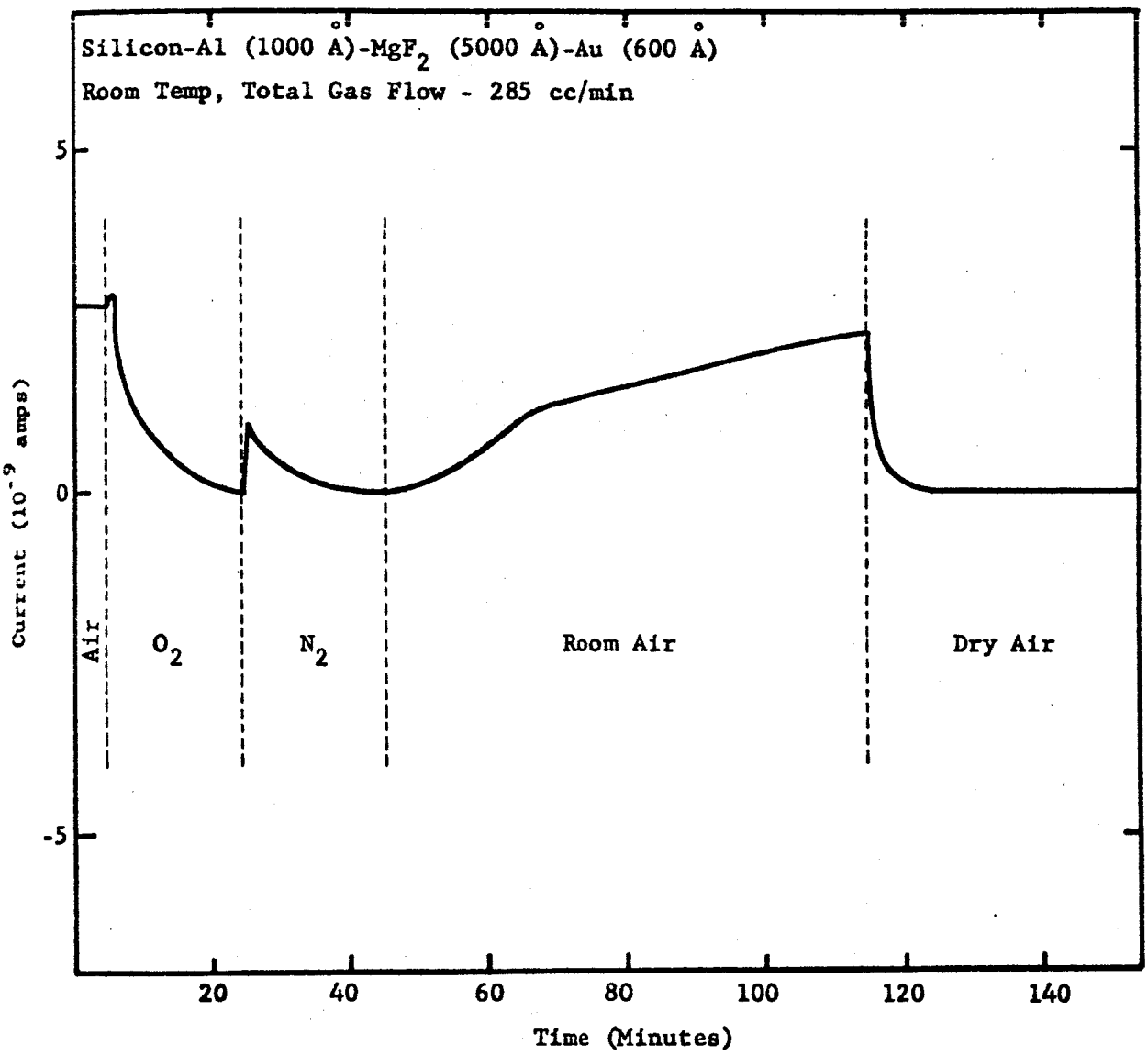

Fig. 16. Short-Circuit Current vs Time in Various Environments

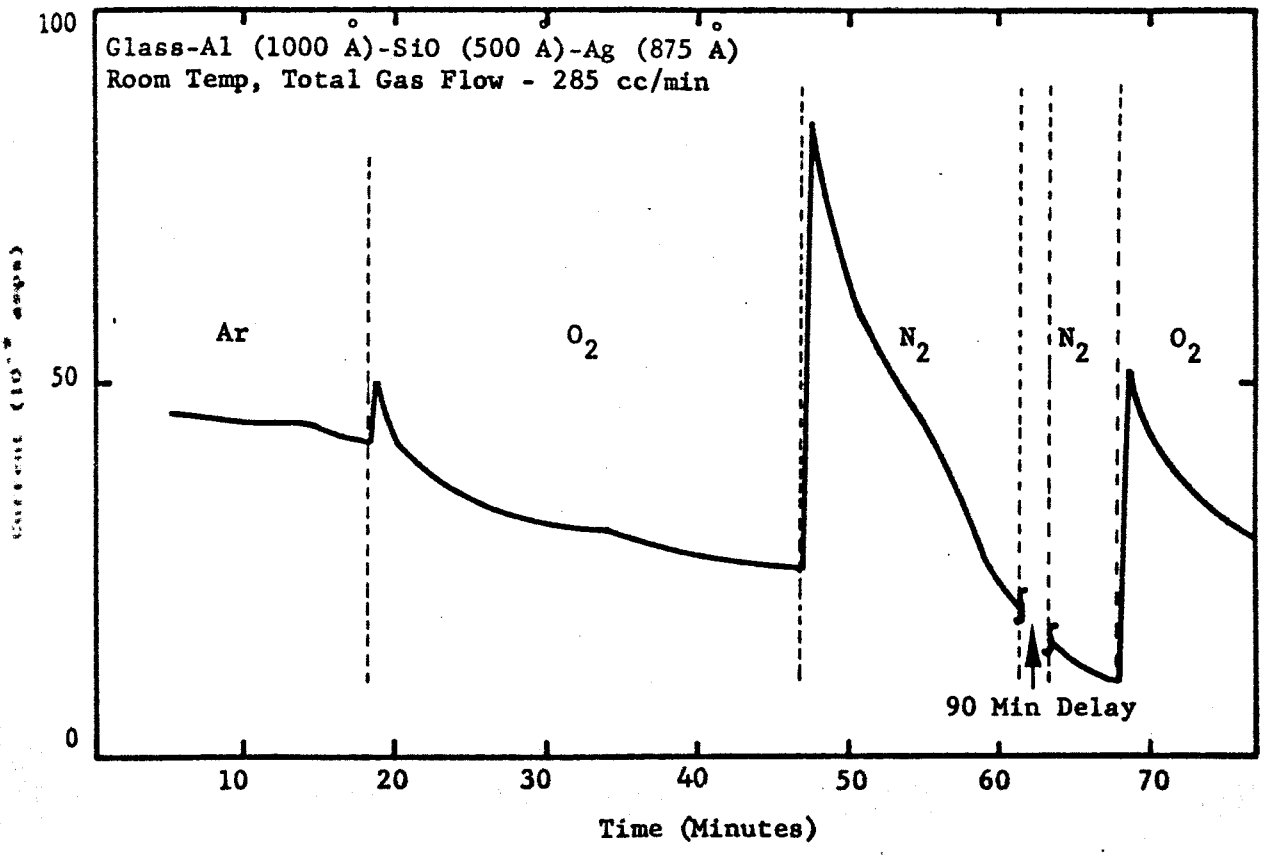

Fig. 17. Short-Circuit Current vs Time for Various Environments

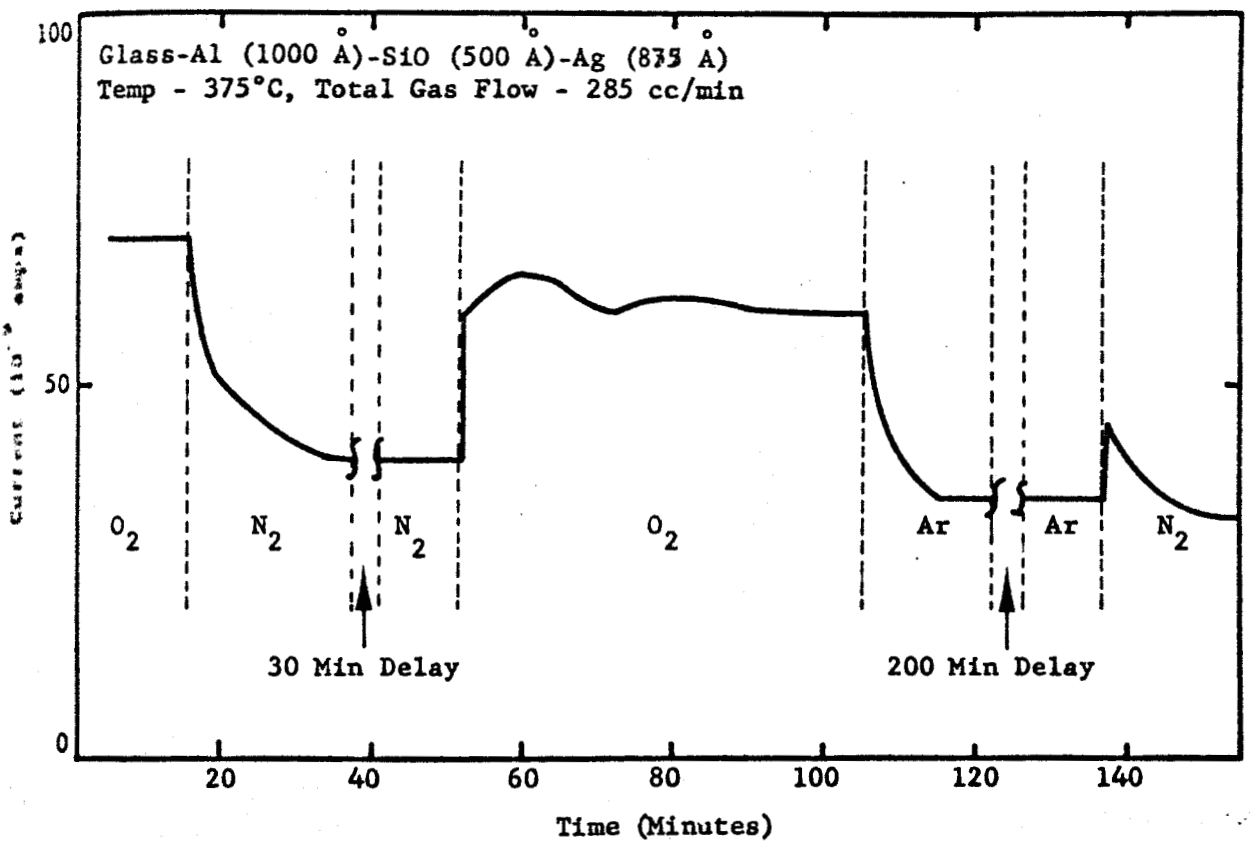

Fig. 18. Short-Circuit Current vs Time in Various Environments

One distinct drawback to this particular structure is its short lifetime due to the oxidation of the top electrode. After being heated to high temperatures, this structure has a lifetime of only about one week. After this time, it becomes increasingly difficult and finally impossible to maintain electrical contact on the silver electrode.

2.2.5 Glass-Copper-Silicon Monoxide-Gold

These structures were manufactured in the geometry shown in Fig. 7. Figure 19 shows the short circuit response to varying partial pressures of oxygen, argon, and nitrogen. In general, this type of sample behaved similar to the Al-SiO-Au structure.

As can be seen from Fig. 19, the short-circuit current was about 0.4 nanoampere in oxygen at atmospheric pressure as compared to about 0.2 nanoampere for argon and nitrogen at the same pressure. The difference in current output between vacuum and the inert gases is believed to be due to surface characteristics of the thin films and not to the galvano-diffusion effect. The range of temperature operation for the Cu-SiO-Au samples was about 200°C to 300°C.

2.2.6 Glass-Gold-Lead-Silicon Monoxide-Gold

These structures were manufactured in the cross-stripe geometry by evaporating a 750 Å layer of gold onto a glass slide, evaporating a 1000 Å layer of lead congruent to the gold, evaporating a square of silicon monoxide over part of the lead stripe, and evaporating a layer of gold over the silicon monoxide perpendicular to the lead. The first layer of gold was for electrical contact purposes only.

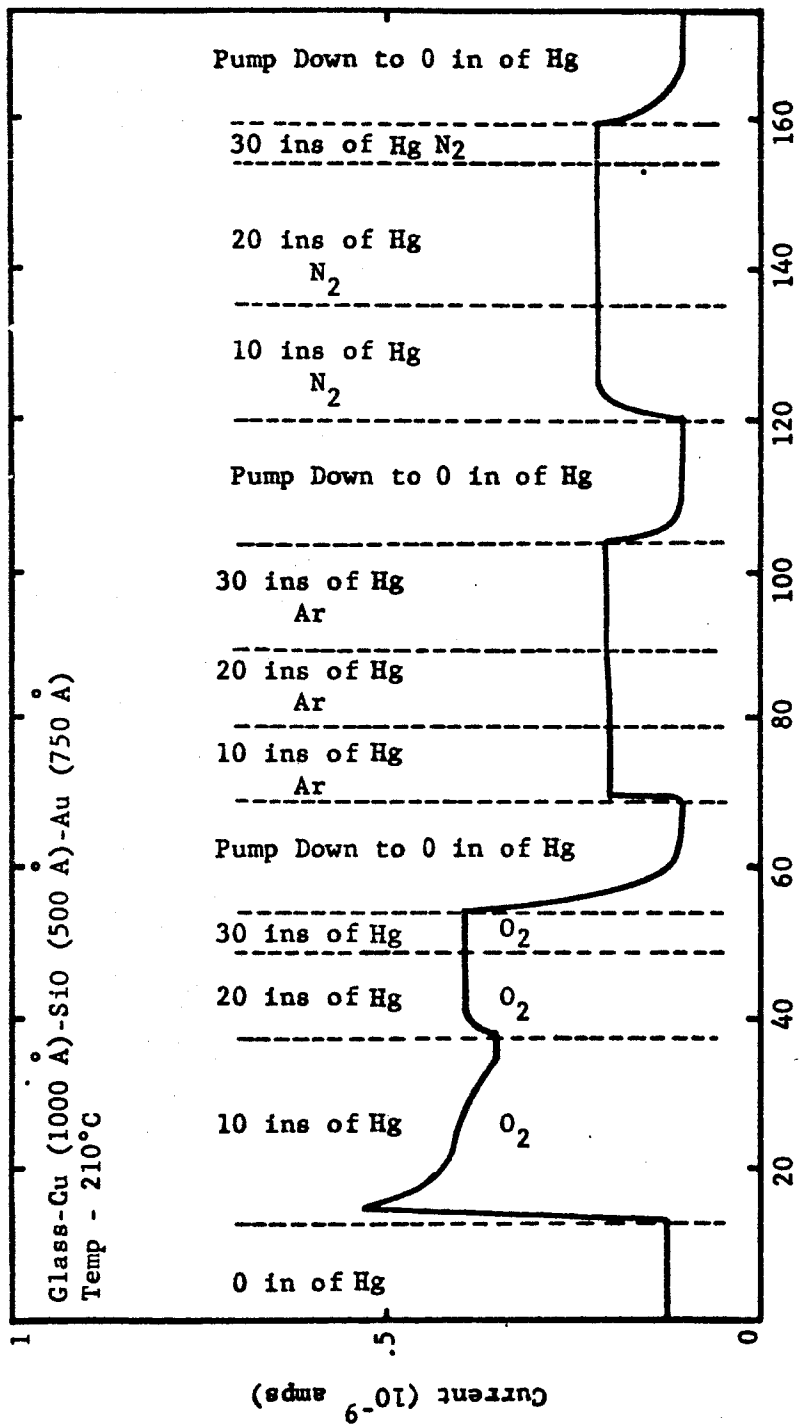

Fig. 19. Short-Circuit Current vs Time for Various Environments

Figure 20 shows the short-circuit current output versus time as a function of various environments. It is seen that the current output is low (10^{-10} amps) and that change in current from an oxygen environment to an inert environment is small.

In some cases this structure exhibited sharp transient currents when exposed to oxygen or nitrogen from a previous environment. The current peaks were positive for oxygen and negative for nitrogen. Figure 21 shows this effect. It was very difficult to obtain consistent data from this type of structure.

2.2.7 Glass-Gold-Bismuth-Silicon Monoxide-Gold

These samples were made similar to the lead samples discussed in the previous section. A layer of gold was again used for contact purposes.

Figure 22 shows the current from this structure as a function of environment and time at a temperature of 240°C. Notice that the steady-state current from the sample in any environment was negative. Also sharp negative peaks were encountered when oxygen was turned off. It is not fully understood why this took place. Although the data for this particular figure was taken at 240°C, this data is typical for runs at 250°C and 340°C.

Figure 23 shows a partial pressure curve for a sample that has the same structure as the one in Fig. 22. Notice that the change in current versus the change in pressure is nearly linear.

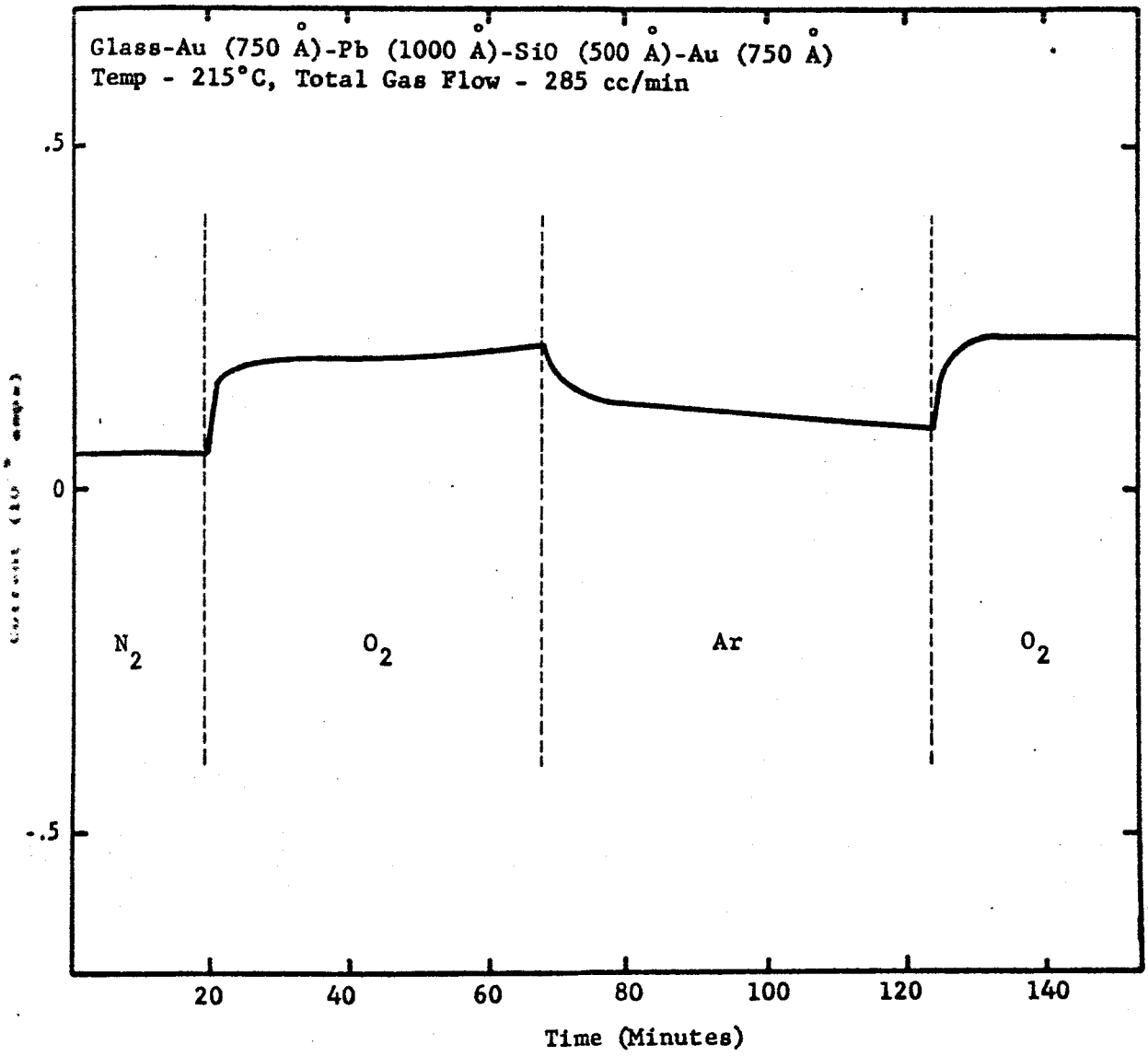

Fig. 20. Short-Circuit Current vs Time in Various Environments

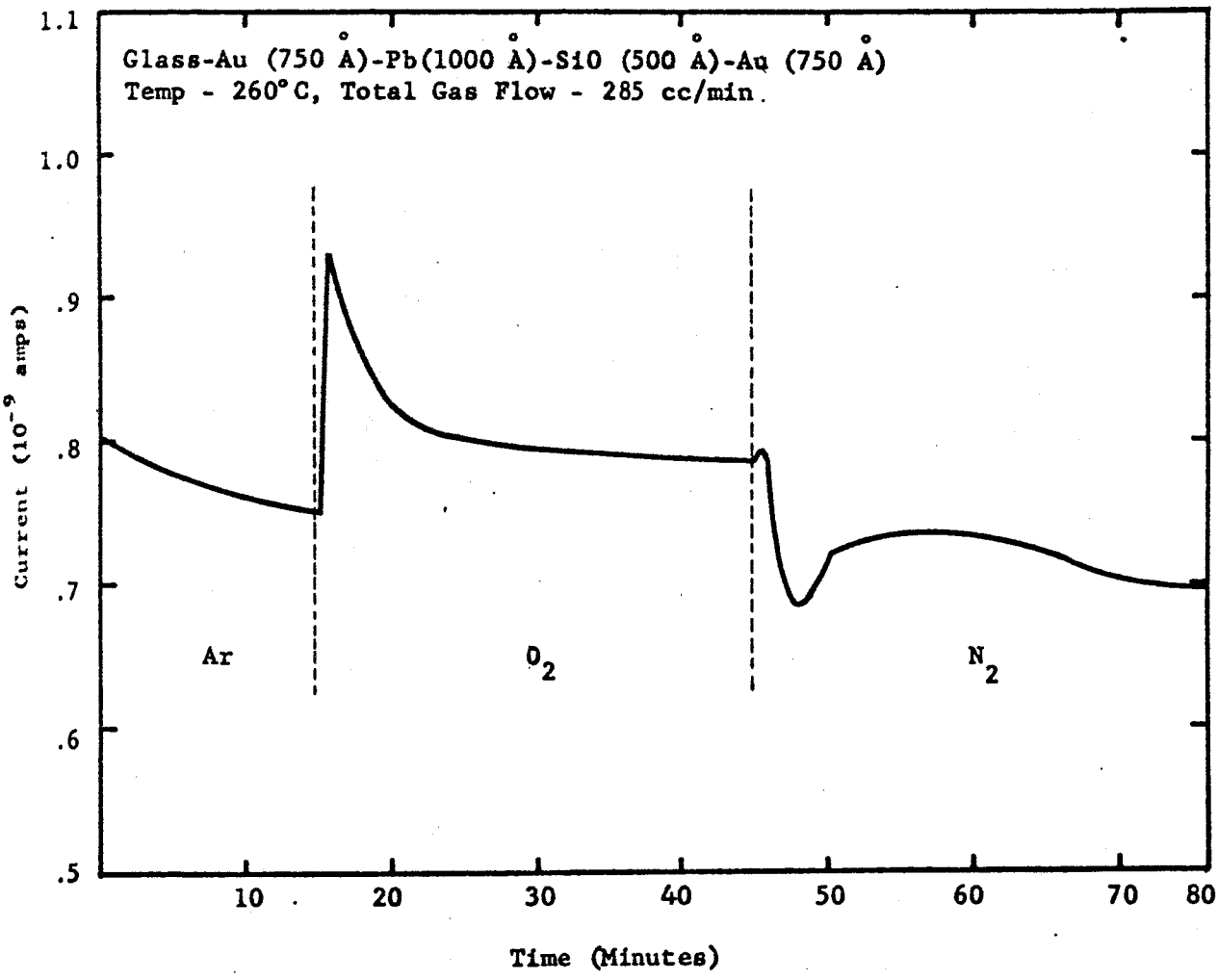

Fig. 21. Short-Circuit Current vs Time in Various Environments

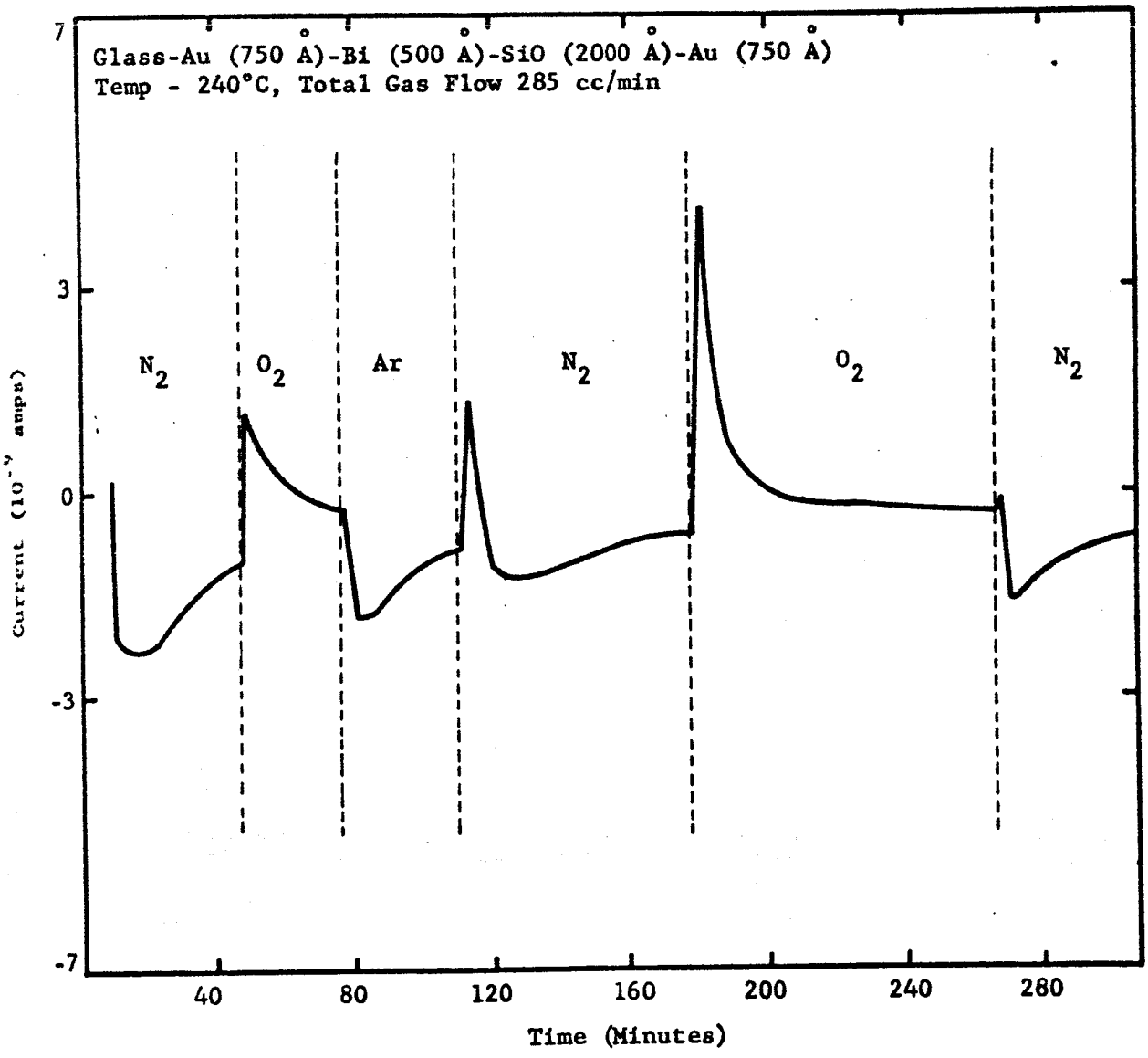

Fig. 22. Short-Circuit Current vs Time in Various Environments

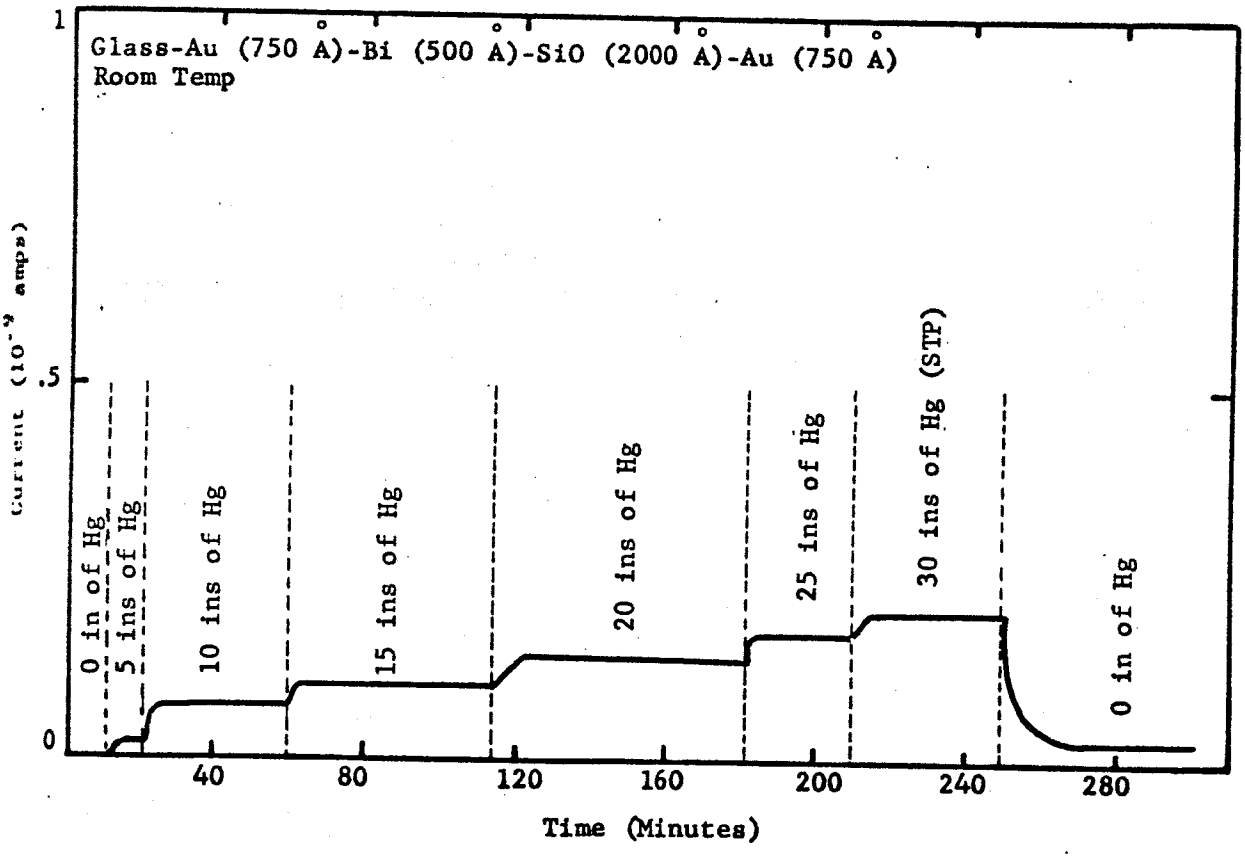

Fig. 23. Short-Circuit Current vs Time for Various Air Pressures

2.2.8 Glass-Gold-Manganese-Silicon Monoxide-Gold

These structures were manufactured by evaporating 750 Å of gold onto a glass slide, 1000 Å of manganese congruent to the gold, 1500 Å of silicon monoxide over the manganese, and 750 Å of gold over the SiO.

In all previous structures the oxidizing electrode had formed a nonconducting oxide, but oxidized manganese forms trimanganese tetraoxide which is a conductor. For this reason a thicker dielectric was needed to prevent samples from being short circuited. The dissipation factor of all manganese structures has been found to increase and the capacitance has been found to increase or change only slightly. This was expected since the dielectric thickness had not changed or had grown thinner due to "fill up" of valleys in the dielectric by conducting oxide growth.

Because of the constant dielectric thickness, it was expected and noted that these structures had better short-circuit current stability than those with nonconducting oxides. In addition, these structures had longer lifetimes than any studied previously. One sample was operated continuously during normal working hours for over one month and was still operatable when removed from the experimental chamber.

Figure 24 shows the relation between oxygen and current output. On account of the thicker dielectric, the current output was less than the current output of many other samples studied. Figures 24 and 25 show typical data for this type of structure at two different temperatures.

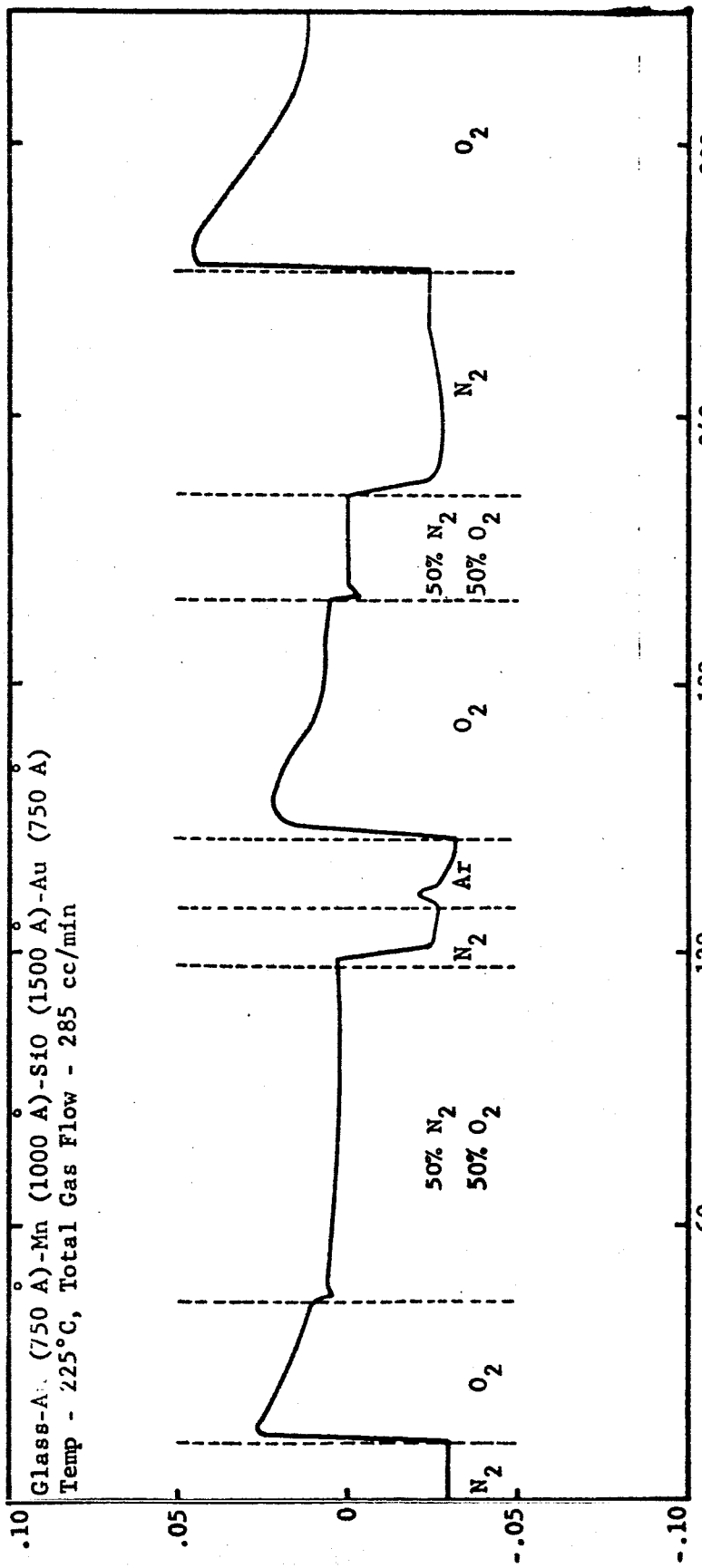

Fig. 24. Short-Circuit Current vs Time in Various Environments

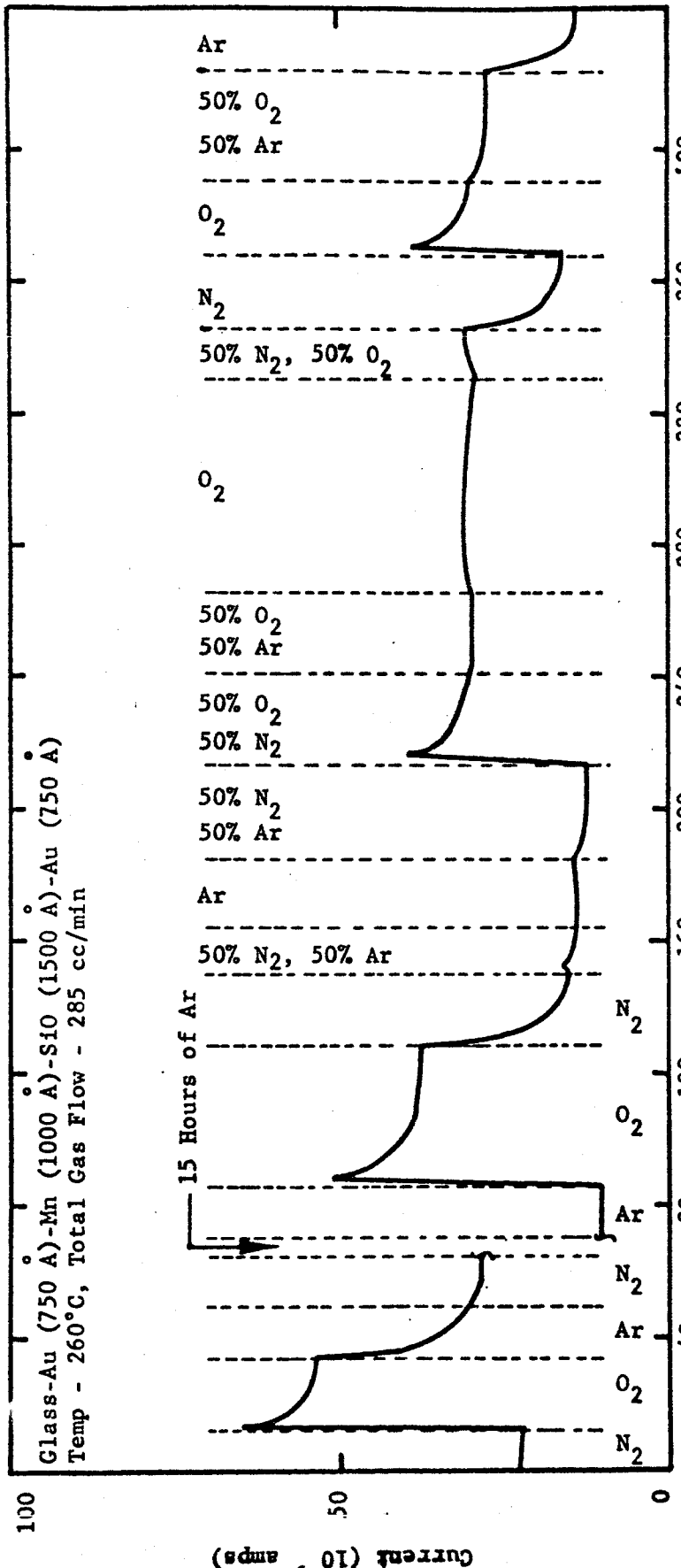

Fig. 25. Short-Circuit Current vs Time for Various Environments

Data was obtained with a constant total flow rate across a given sample, but with varying percentages of oxygen in the flow. Figure 26 shows a plot of short-circuit current versus percentage of oxygen. This percentage of oxygen is analogous to partial pressures of oxygen. It is seen from the graph that the current output is logarithmically related to oxygen partial pressure.

2.2.9 Glass-Manganese-Silicon Monoxide-Manganese

This system had a cross-stripe structure with 1000 Å of manganese on each side of 1500 Å of silicon monoxide. The internal impedance of this sample was only 300 ohms as compared to impedances in the megohm for all other types of samples. Consequently, the capacitance and dissipation factor of these samples could not be measured. At the beginning of the tests, these structures behaved very similar to the Glass-Au-Mn-SiO-Au samples. However, after three days of operation, the polarity of the samples reversed and negative current output was observed in 100 percent oxygen.

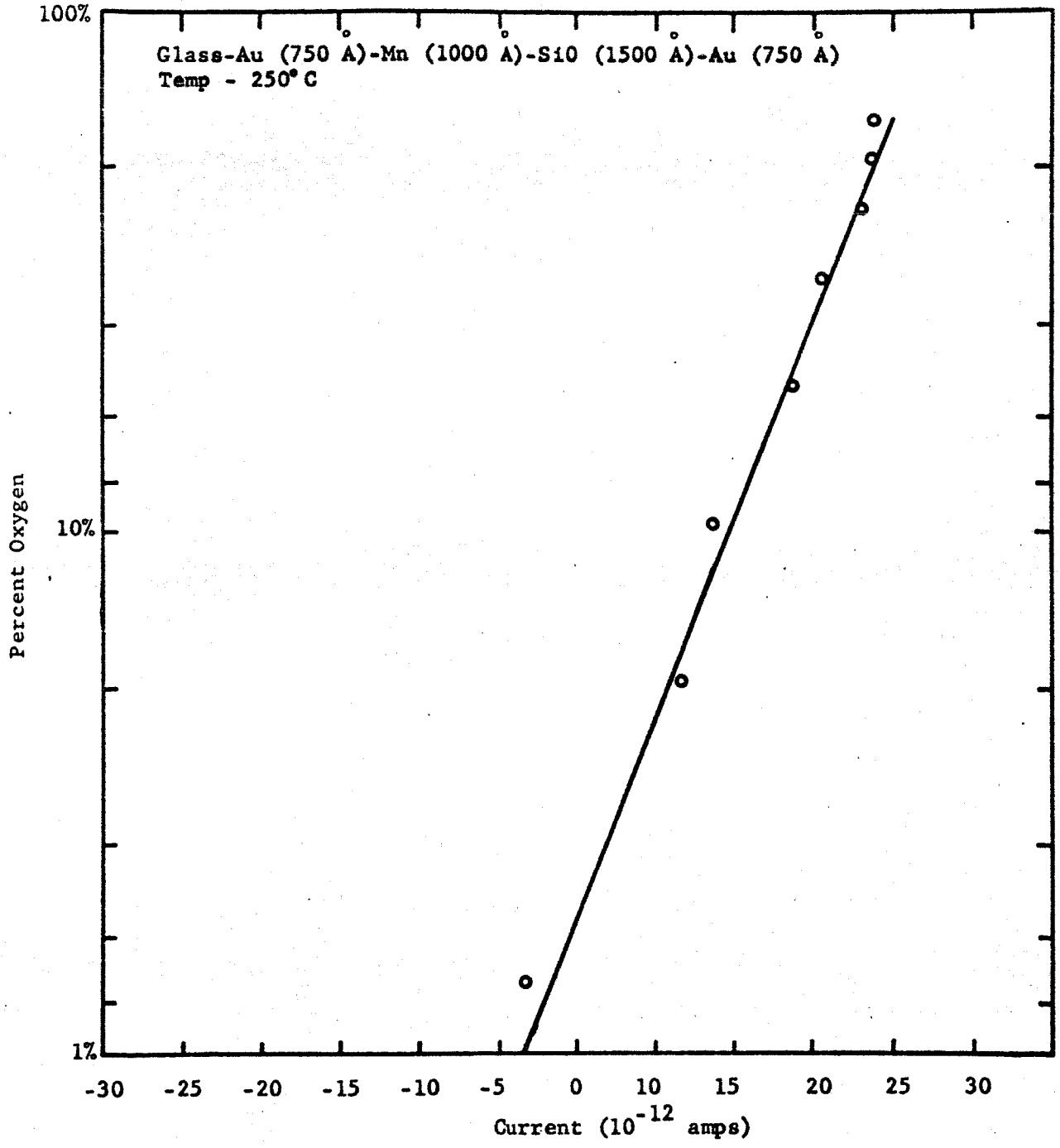

Fig. 26. Short-Circuit Current vs Oxygen Partial Pressure

2.3 Summary

Support for the theoretical model of galvano-diffusion is found in the change in capacitance and dissipation factor with operating time. In all cases, except for samples with manganese as the oxidizable electrode (as previously discussed), the capacitance and dissipation factor decreased during measurements. This results from the increase in dielectric thickness with the oxidation of the bottom electrode since all structures studied, except manganese, formed insulating oxides. The capacitance of a parallel plate capacitor is

$$C = 0.0885 \, \kappa \frac{A}{L} , \tag{22}$$

where C is the capacitance in picofarads, κ is the dielectric constant relative to air, A is the area of one plate in square centimeters, and L is the dielectric thickness. The above equation can be written as

$$C = \frac{K}{L} , \tag{23}$$

where K is a constant. As can be seen from the above equation, the capacitance decreases as the thickness of the dielectric increases. This assumes that the dielectric constant is constant.

One can also reason that the dissipation factor should improve or decrease with the growth of a nonconducting oxide since the evaporated dielectric has valleys and pinholes which can be filled by the oxide before the thicker portions change. Table 1 gives quantitative data on some of the samples tested.

Table 1

Capacitance Data

Sample Number	Top Electrode	Å Thick	Dielectric	Å Thick	Bottom Electrode	Å Thick	Capacitance (nf) Before	After	Dissipation Factor Before	After
020465-1	Au	500	SiO	5000	Al	1000	6.50	4.970	.05	.193
020565-1	Au	500	SiO	10000	Al	1000	2.80	2.196	.054	.0025
021865-1	Au	500	MgF_2	5000	Al	1000	52.52	14.18	.63	.38
021865-2	Au	500	MgF_2	5000	Al	1000	31.68	23.92	.37	.41
022465-1	Au	500	MgF_2	5000	Al	1000	40.80	4.53	.71	.147
030165-1	Au	600	MgF_2	5000	Al	1000	6.78	5.58	.235	.077
030965-1	Au	700	MgF_2	4000	Al	1000	53.35	6.6	.71	.106
031665-3A	Au	700	MgF_2	4000	Al	1000	1.730	1.151	.127	.0064
050365-4A	Au	750	SiO	500	Au & Bi	2000	5.33	1.503	.40	.047
051165-1B	Ag	875	SiO	500	Al	1000	8.085	4.301	.095	.012
060465-3A	Au	750	SiO	500	Au & Pb	750 & 1000	1.603	1.489	.005	.0013
060465-2D	Au	750	SiO	500	Au & Pb	750 & 1000	1.957	.558	.005	.003
061065-2A	Au	750	SiO	500	Al	1000	2.508	1.296	.057	.001
061065-3A	Au	750	SiO	500	Al	1000	1.975	1.305	.035	.006
061065-2B	Au	750	SiO	500	Al	1000	2.786	1.563	.056	.0125
061065-2C	Au	750	SiO	500	Al	1000	2.499	1.323	.056	.0025
062565-3A	Au	750	SiO	500	Cu	1000	5.832	.032	.0245	.005
072665-3D	Au	750	SiO	1500	Au & Mn	750 & 1000	1.906	2.800	.011	.76
072665-3B	Au	750	SiO	1500	Au & Mn	1000 & 750	1.954	1.766	.0175	.075
072665-3A	Au	750	SiO	1500	Au & Mn	1000 & 750	1.847	1.700	.052	.27

By the same reasoning the growth of a conducting oxide should increase the dissipation factor by diffusing into the pinholes. The capacitance should not change unless the effective thickness of the dielectric decreased by the filling of holes and valleys with a conductor thereby giving an increased capacitance. It is therefore not surprising that of the structures studied Mn-SiO-Au was the most stable with respect to time since manganese oxide is a conductor.

Attempts to enhance or retard the process by applying an external potential to the devices were unsuccessful. The results were not consistent between like samples. The general conclusion reached was that electronic leakage increased greatly with applied field.

Though all structures studied exhibited the galvano-diffusion effect and were thereby oxygen partial pressure sensors, some are preferable over others. Magnesium fluoride and aluminum oxide were found to result in devices which were extremely sensitive to water vapor. Factors other than these dielectrics could have influenced this, such as geometry. Glass-Al-SiO-Ag structures have a very short lifetime due to the oxidation of the Ag and could be used only over periods of time of a week or less. The glass-Au-Pb-SiO-Au and glass-Au-Bi-SiO-Au structures were found to be erratic in behavior, possibly because of low free energy of formation of Pb and Bi. The free energy of formation is -43 kcal/g-mole and -120 kcal/g-mole for lead oxide and dibismuth trioxide respectively. For comparison, the two structures that presented the best data from the viewpoints of age, stability, oxygen sensitivity, and nonerratic behavior were aluminum and manganese. Their free energies of formation are -380 kcal/g-mole for dialuminum trioxide and -300 kcal/g-mole for trimanganese tetraoxide.

The ionic concentration at the oxide-dielectric (interface 2) is directly related to the negativity of the free energy of oxide formation. The ionic concentration is expected to be smaller for aluminum or manganese as the oxidizable electrode, and consequently more electronic current should flow in the external circuit. Since dicopper oxide and copper oxide have free energies of formation of -27 and -32 kcal/g-mole respectively, they fall into the same category as bismuth and lead.

The two structures that seem most desirable for oxygen sensors are glass-Al-SiO-Au and glass-Mn-SiO-Au. The conclusion is verified by the experimental results.

There is a possibility of combining the desirable effects of both the aluminum and manganese properties into one structure. As previously stated, dissipation factors of aluminum electrode structures improve with time, and the capacitance and short-circuit current of manganese electrode samples are approximately constant with time. Therefore a structure that utilizes manganese covered by a very thin layer of aluminum (approximately 30 Å) could possible exhibit both desirable properties after short operation times.

3. CONDUCTANCE MODULATION

Conductance modulation, as used here, means a change or modulation of the electrical conductance of a thin film that is induced or results from changes in the environmental gas and its pressure. The term adsorption is taken to mean the process whereby gas atoms or molecules are attached to the surface of the film. Sorption is taken to mean the process whereby gas atoms or molecules are absorbed into the bulk of the film. Using these definitions, there are then two ways environmental gases can change the electrical conductance: (1) by adsorption and evaporation and (2) by sorption and desorption. The amount of a particular gas that is either adsorbed on the surface or located in the bulk is a function of the film material, the type of gas, and the partial pressure of the gas. It is, of course, the latter property that is of interest here, and in particular, it is the conductance as a function of the oxygen partial pressure.

3.1 Discussion

Consider first the interactions with the surface only (adsorption and evaporation). When interacting with the surface the mechanism can be either chemical bonding or Van der Waal force. For the present no differentation is made between the two. Generally speaking, if a clean surface is exposed to a gas environment, gas adsorbs on the surface and increases the electrical resistance. For example it has been found that the decrease in film conductance depends upon the number of molecules adsorbed on the film and is given by [7,8]

$$\frac{\Delta\sigma}{\sigma} = -\alpha(n/N) \ , \qquad (24)$$

where σ = conductivity of the clean film

n = number of adsorbed molecules

N = number of metal atoms in the film

α = a small number (approximately 2 for oxygen).

This model is based on the assumption that a number α of conduction electrons are deactivated by each adsorbed molecule. Chemical bonding is implied with the above assumption.

Another model which has not been considered previously is the effect of adsorbed gas on the specular or diffuse scattering at the surface of the film. Specular scattering is defined as that which occurs when the velocity component of an electron moving normal to the surface is reversed and the transverse component of velocity is unchanged. In diffuse scattering the average drift velocity after collision with the surface is zero. Sondheimer has developed the following analytical expression for the effects of surface scattering [9]

$$\frac{\rho}{\rho_o} = 1 + K(1 - P)L/d \ , \qquad (25)$$

where ρ = resistivity

ρ_o = bulk resistivity

d = film thickness

L = electron mean free path in the bulk material

P = fraction of conduction electrons specularly scattered at the surface

K = a constant.

The factor P is a constant which statistically describes the interaction between the conduction electrons and the surface of the film. It represents the fraction of electrons specularly scattered at the surface (P varies between 0 and 1). It is this factor that can be affected by the adsorbed gases.

It has been found experimentally, during the course of the present study, that the conductance of gold films is a function of the oxygen partial pressure. In particular it has been found that the resistance at an elevated temperature of approximately 200°C, reversibly decreases about 4 percent when the environment is cycled from an inert gas to oxygen. It is believed that this decreased resistance results from changes in the sacttering at the surface. The effect is a function of temperature as will be discussed later.

The question as to why oxygen affects the surface scattering processes differently from nitrogen or argon is not immediately obvious. It is suspected that oxygen adsorbed on the surface may form gold oxide whereas nitrogen and other inert gases may not react chemically. This introduces several possibilities for conductance changes. For example, the number of charge carriers may change as described by the previous model. Competing processes may take place.

Generally speaking gold does not oxidize readily. It is possible to anodize gold in perchloric acid [10]. Electron micrograph studies by Guinpl, McMaster and Freschillo have shown that gold films 400 Å thick are covered with thin membrane layers [11]. They speculate that these amorphous layers may be gold oxide. If only a monolayer of oxide is formed, one would expect the surface properties to change. Oxide formation is not inconsistent with reversible changes since gold oxides

are unstable at the temperatures required to observe the effect (120°C to 250°C). All known oxides of gold decompose at temperatures greater than 205°C.

Other models for the effects of adsorbed gases on conductance have been proposed [12]. Unlike the above models which assumed a uniform surface on the film, a common assumption is that the film is made up of a regular array of individual metal blocks separated from one another by a gap. This gap is partly filled by a metal layer. Based on this picture of the film, adsorbed molecules could alter the conductance of the film by the following processes.

1. The conduction of both the blocks and bridges may be altered by a surface effect such as those already mentioned.
2. Surface stresses in the film may be affected by adsorption, thereby changing the resistance.
3. If the thickness of the metal bridges, as well as the gap width, is small, current flow may occur by tunneling through the gaps. Adsorption on the gap walls may affect the surface dipole layer and therefore also affect conduction across the gap.

Still another model has been proposed to explain the effects of transient or pulsed oxygen adsorption on NiO surfaces [13]. This theory is based on multiple-trapping involving excited oxygen atoms or molecules and ionized species.

The adsorption of gases onto the surfaces of thin films which result only in surface changes must almost by necessity occur at low temperatures--on the order of a few hundred degrees centigrade or less. This is because at high temperatures the diffusion of the adsorbents into

the film will be high. This can be seen from the discussions in Section 2. In general oxygen will be adsorbed onto the surfaces of metals by chemical bonding. Unless noble metals are used for the film, oxides will be formed and the process will be irreversible at low temperatures where the oxides are stable. This reduces considerably the possibilities of utilizing only surface adsorption effects involving oxygen.

Attention is now focused on sorption or diffusion of environmental gases into the film. As already mentioned, one expects these effects to occur more readily at high temperatures. Discussion of irreversible oxidation of the bulk film will be deferred to Section 4.

Conduction can be changed by sorption or desorption of materials that enhance or decrease the number of charge carriers or alter the mobility of the carriers. Semi-insulators or wide band gap semiconductors of the metal oxide type appear promising where the environmental gas is oxygen. In these materials an excess or deficiency of oxygen can result in orders of magnitude changes in the conductivity from its normal value. Hafnium, zirconium and titanium oxides are notable for the above properties.

Rutal (TiO_2) has been the subject of many investigations in the oxygen pressure range of from 1 atmosphere to 10^{-12} atmospheres [14,15]. Figure 27 shows a plot of $\log_{10} P(O_2)$ (atm) as a function of conductivity for TiO_2 [15]. From the data it is seen that

$$\sigma = K(T)\,[P(O_2)]^{-1/5} , \qquad (26)$$

where K(T) is a constant. Based on the -1/5 power pressure dependence it has been concluded that titanium ions are the dominant defects [15].

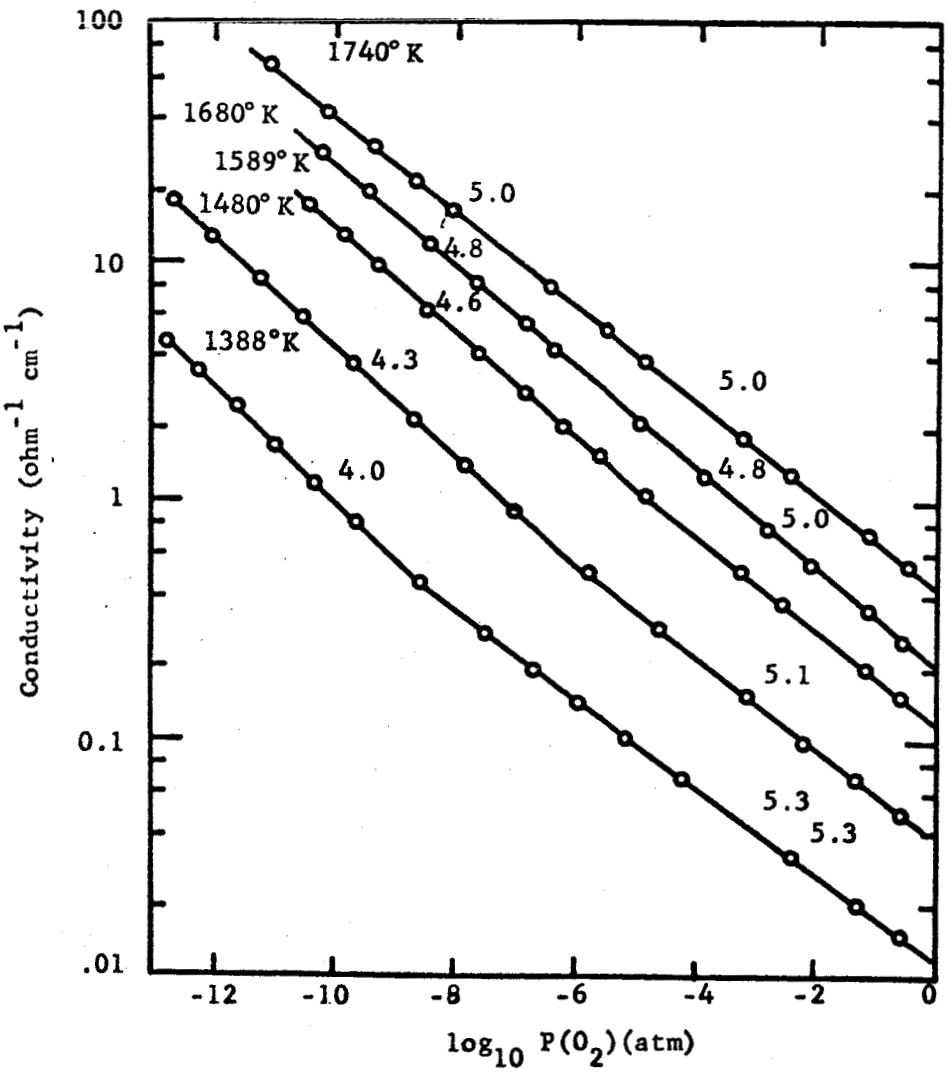

Fig. 27. Conductivity of TiO_2 as a Function of Oxygen Partial Pressure

Other investigations have given the power term as -1/6 [16]. This dependence has been explained in terms of oxygen vacancies.

The electrical conductance of ZrO_2 at elevated temperature (> 900°) has been found to be a function of oxygen partial pressure [17,18,19]. The crystal structure of the material strongly influences the dependence of conductance on oxygen partial pressure--monoclinic crystals are more oxygen sensitive than tetragonal crystals. Figure 28 shows a plot of log σ vs log oxygen partial pressure for the two crystal types at various temperatures [17]. Conductivity is again related to oxygen partial pressure by

$$\sigma = K(T)\ P(O_2)^{1/n}\ , \qquad (27)$$

where n is constant depending on the pressure (see Fig. 28). This dependence has been attributed to oxygen vacancies and interstitials. There is some disagreement as to the extent of ionic and electronic contribution to the total conductivity [17,18]. It has also been found that approximately 5 percent of the total adsorbed oxygen can be reversibly adsorbed and desorbed as molecules [15,21]. The adsorption is theorized to take place on O_2^- ions which are mobile [20,21].

Hafnium oxide (HfO_2) is very similar in its properties to ZrO_2. Figure 29 shows a plot of conductivity as a function of oxygen partial pressure at various elevated temperatures [17]. Here the temperature is lower (> 900°C) than that used in ZrO_2. As shown in the figure the conductance increases to a maximum value when decreases as oxygen partial pressure is lowered. Oxygen vacancies and interstitials are again responsible for the effects.

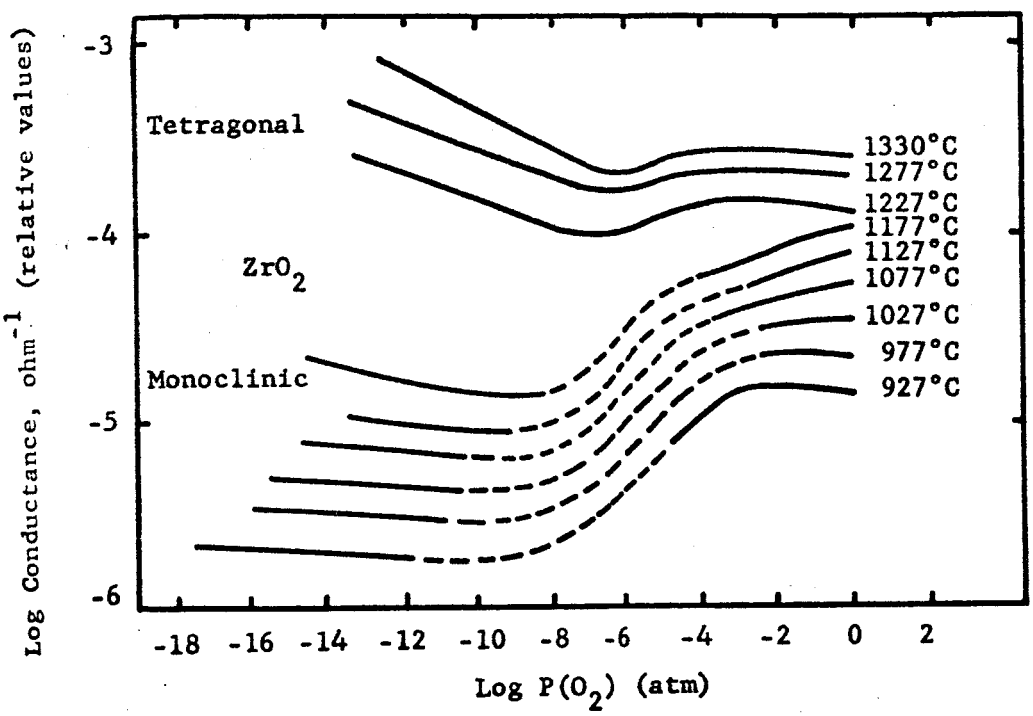

Fig. 28. Conductance of the ZrO_2 Specimen as a Function of the Partial Pressure of Oxygen

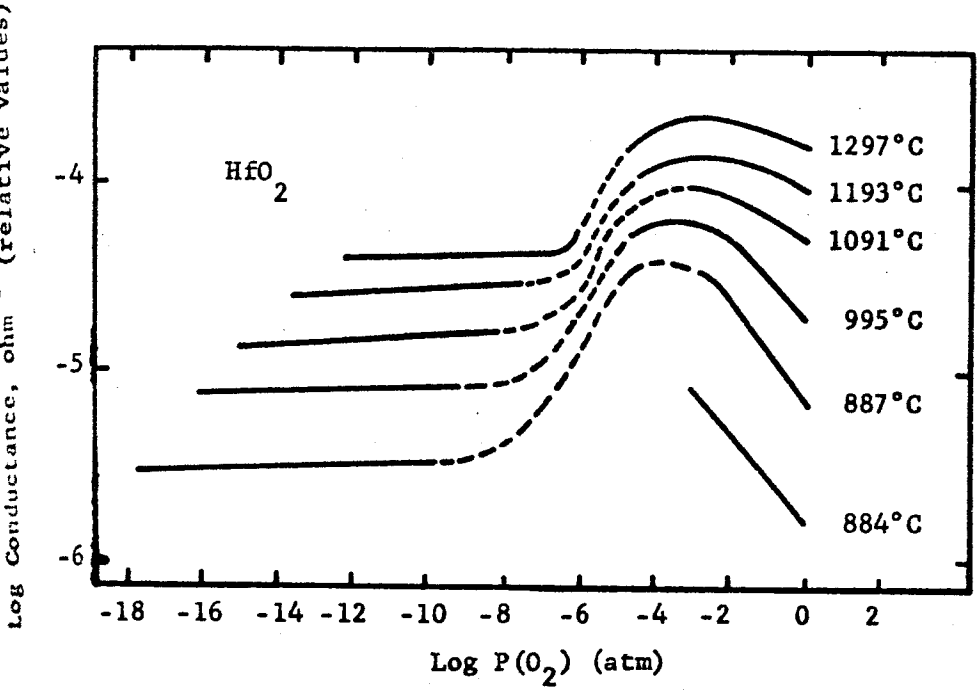

Fig. 29. Conductance of the HfO_2 Specimen as a Function of the Partial Pressure of Oxygen

There are several very detrimental factors which must be considered if one utilizes the above materials as oxygen partial pressure sensors. First the temperatures required are large (~ 1000°C). This is necessary to activate the charge carriers and to enhance the diffusion of oxygen in the film. Second the conductance change is small in the pressure range 0 to 300 mm Hg. Finally the time constants involved in pressure changes are long (hours to days).

3.2 Experimental Techniques

In order to fabricate structures to study the electrical conductance modulation, a thin film of metal was evaporated onto a glass slide. On most of the slides DuPont liquid bright gold was fired onto the silicon for contact purposes before evaporation of the material to be studied. The firing operation was done in an oven at 400°C for at least two hours (see Fig. 30).

The glass slides were cleaned by the procedure outlined in Section 2.3. Most slides were pyrex, but a few used in high temperature experiments were quartz.

The materials studied were hafnium, gold, zirconium, titanium manganese, silver, and nickel. Gold, silver, and manganese were evaporated by standard techniques as described by Ref. 6. In order to evaporate hafnium, zirconium, titanium, and nickel, an electron vapor deposition gun was employed (Materials Research Corporation Model V4-200). The gun was mounted in a Ultek ultra-high vacuum system capable of pressures as low as 5×10^{-9} torr (see Figs. 31 and 32).

Hafnium and zirconium proved difficult to evaporate. One of the first problems encountered was the alloying of the metal into the

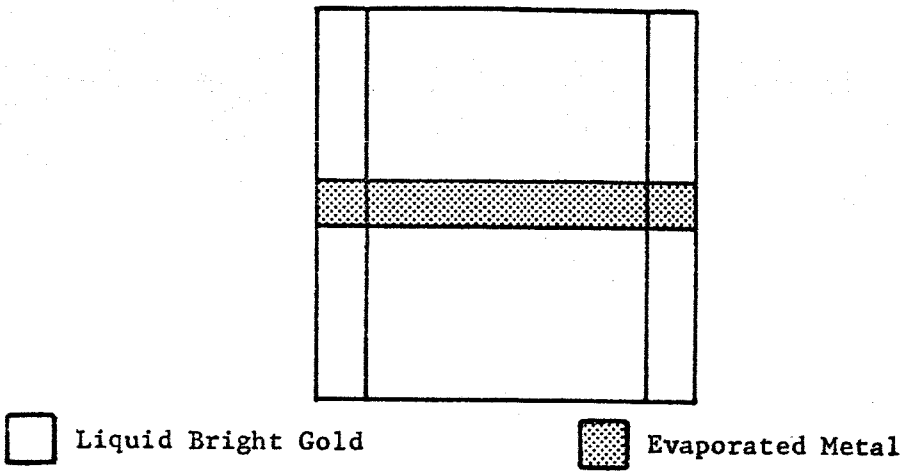

Fig. 30. Geometry of Conductivity Modulation Oxygen Sensor

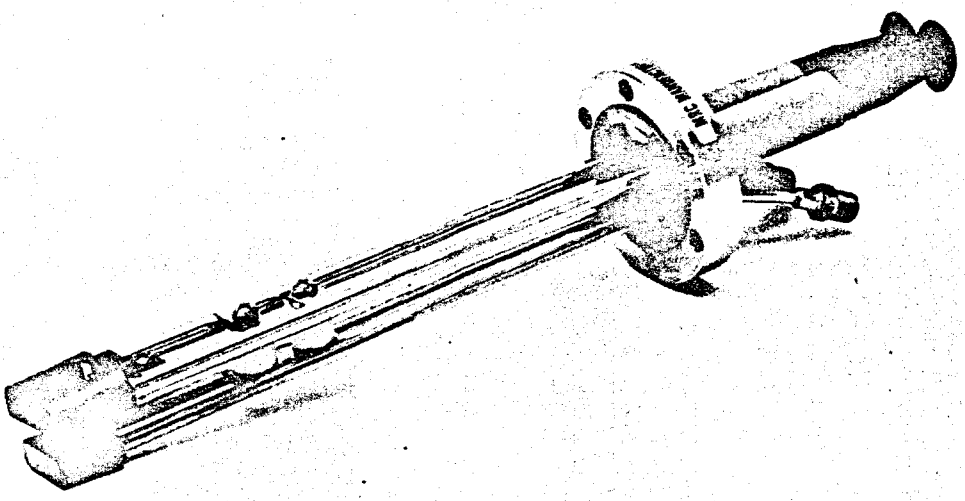

Fig. 31. Electron Beam Vapor Deposition Gun

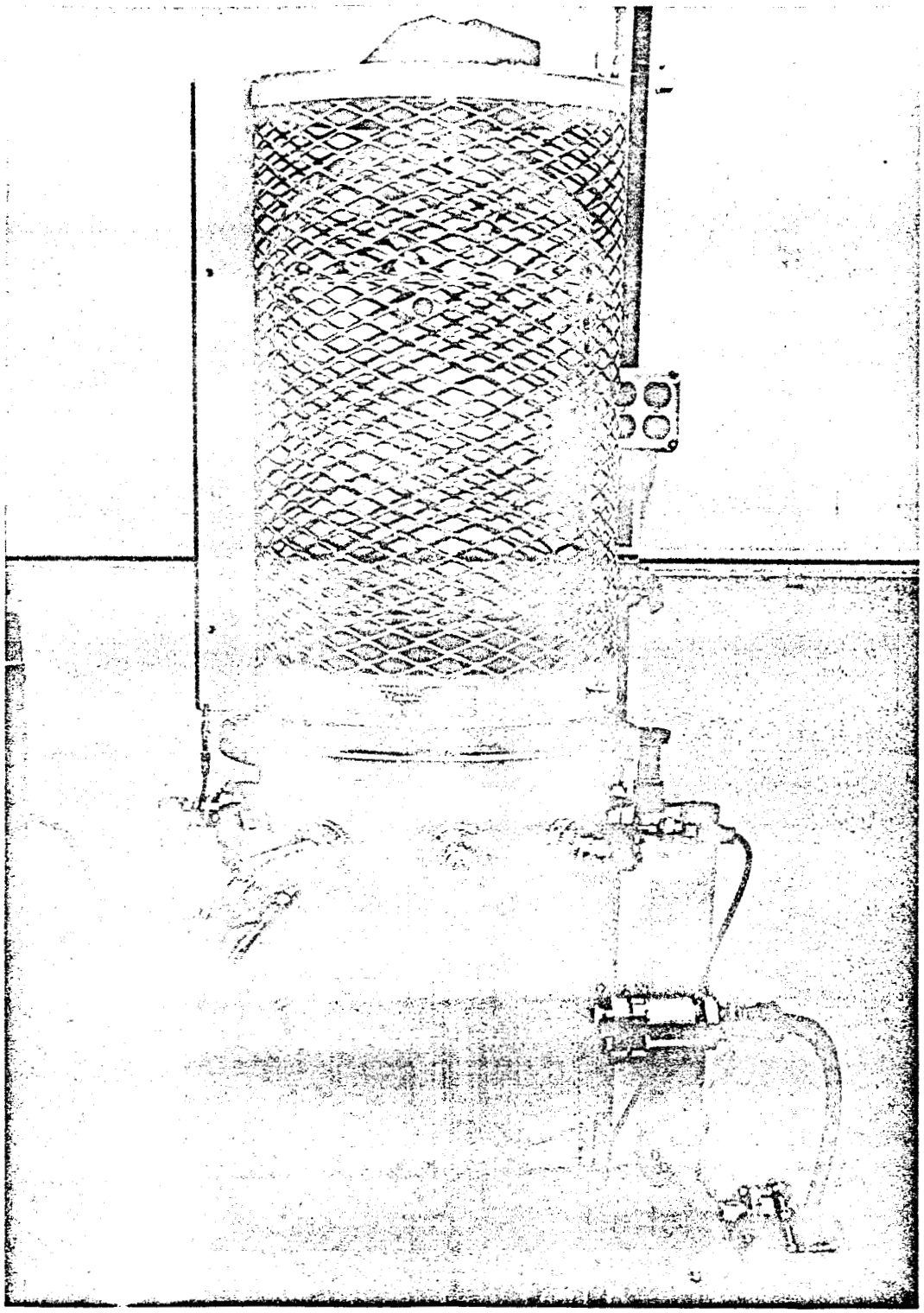

Fig. 32. Electron Gun Mounted in High Vacuum System

water-cooled copper pedestal on which it rested. When the pedestal was covered by a carbon crucible, carbon was evaporated. Finally a procedure was established that yielded good evaporation for hafnium. The procedure as outlined by a typical evaporation was:

1. A carbon crucible containing the hafnium was placed on the copper pedestal of the electron gun. Prior to evaporation the vacuum system was pumped down to a pressure of 5×10^{-8} torr.
2. The hafnium was outgassed at a pressure that ranged from 1.5×10^{-7} to 4×10^{-7} torr for four hours. The power supplied to the electron gun was 2000 volts at 50 milliamps. The temperature of the hafnium as measured by a Leeds and Northrup optical pyrometer was 1360°C.
3. At the end of four hours of outgassing, the voltage and current to the electron gun was slowly increased. The hafnium started melting at approximately 3000 volts and 110 milliamps; the measured temperature was 1990°C. The pressure typically increased to 9×10^{-7} torr during the power increase.
4. The power was increased further to 4000 volts and 200 milliamps with the measured temperature at 2240°C. At this time the substrates were rotated over the source.
5. The total evaporation time was 22 minutes at 2240°C. The pressure during evaporation was 2.2×10^{-6} torr.

Although the thicknesses of these films were not monitored during evaporation, later measurements showed most films to be between 400 Å and 500 Å.

Zirconium, titanium, and nickel were evaporated by the electron gun using the same procedure. Because of the lower melting points of titanium and nickel, not as much power was needed to evaporate them; only about 2500 volts at 100 milliamps. Once the films had been prepared for study, they were stored in a vacuum until used.

The first method utilized for measuring the resistance of the sample was the Wheatstone bridge. Figure 33 shows an electrical schematic of the bridge used. R_x was designated as the resistance of the film whose electrical conductivity was expected to change due to variations in oxygen partial pressures. In some cases R_R was an evaporated film of the same type as R_x. R_R was masked from the environmental changes by a thick coat of Dow-Corning varnish or evaporated SiO. This was to provide temperature compensation to the bridge since R_R and R_x were in opposite legs of the bridge.

The bridge output current (I_3) was recorded using either a Bausch and Lomb or Heathkit recorder. R_x and R_R for the evaporated films mentioned in this reaction were always less than 500 ohms and most of the time less than 100 ohms. The ohmic values of P and Q were selected to be close to the values of R_x and R_R. The change in the sample resistance is related to the potential difference between nodes A and B (ΔV) by

$$\Delta R_x = \frac{\Delta V(R_R R_x + R_x Q + PQ + R_R P)}{-QE}. \qquad (28)$$

The second method used to study the change in resistance of thin film was the four point probe as depicted by Fig. 34. Figure 35 shows the four-point probe used in the tube oven experimental chamber.

DC Micro-Volt Ammeter

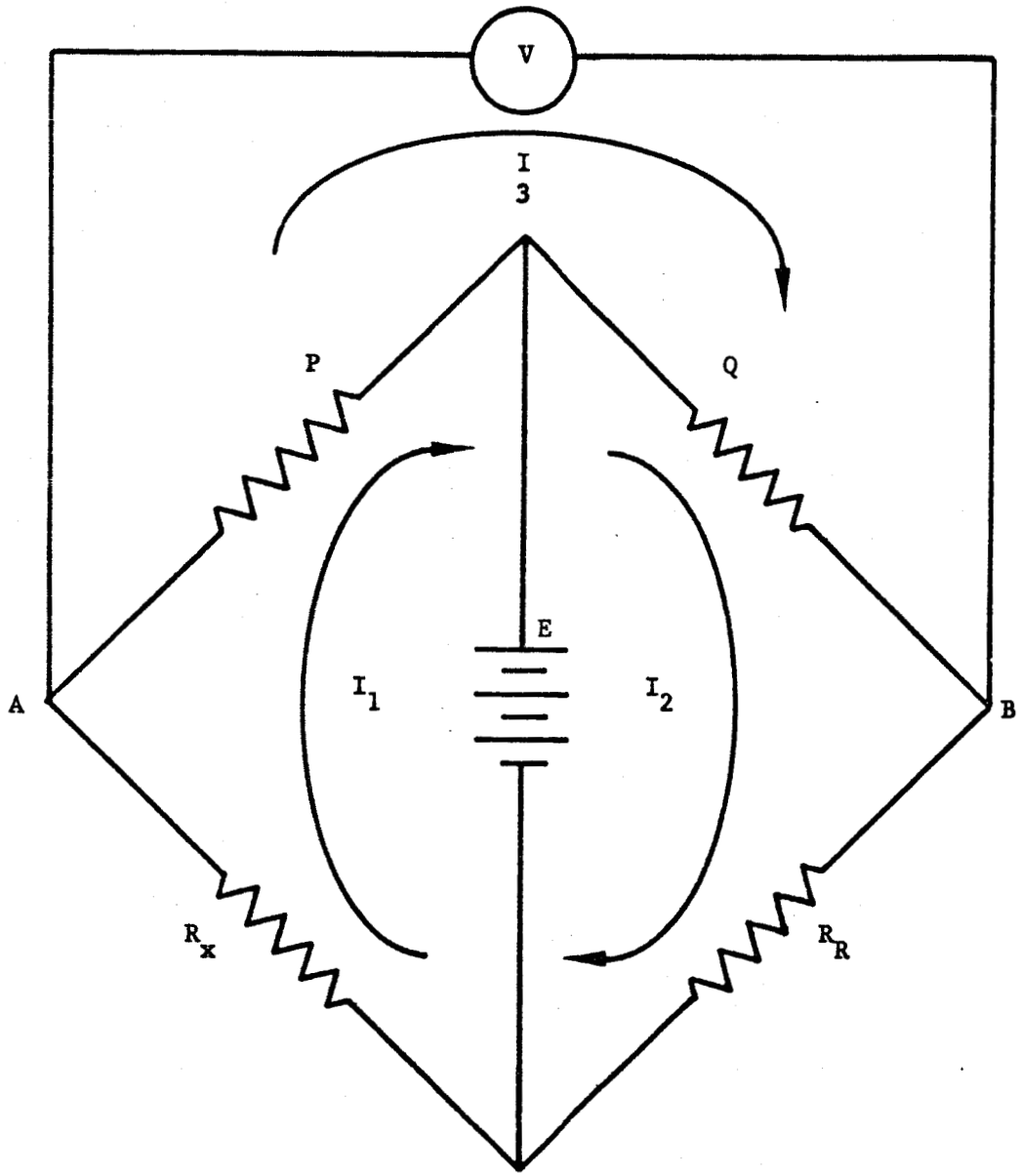

Fig. 33. Schematic of Wheatstone Bridge

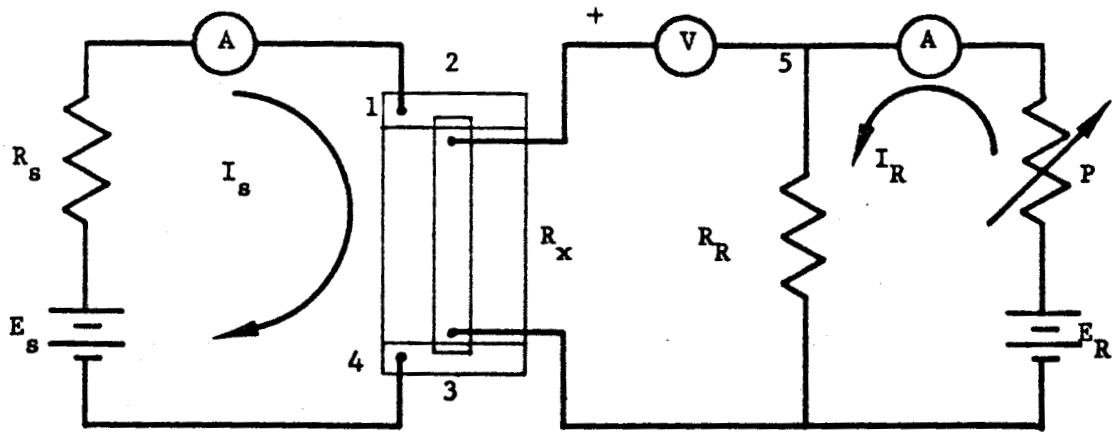

Fig. 34. Schematic of Four-Point Probe

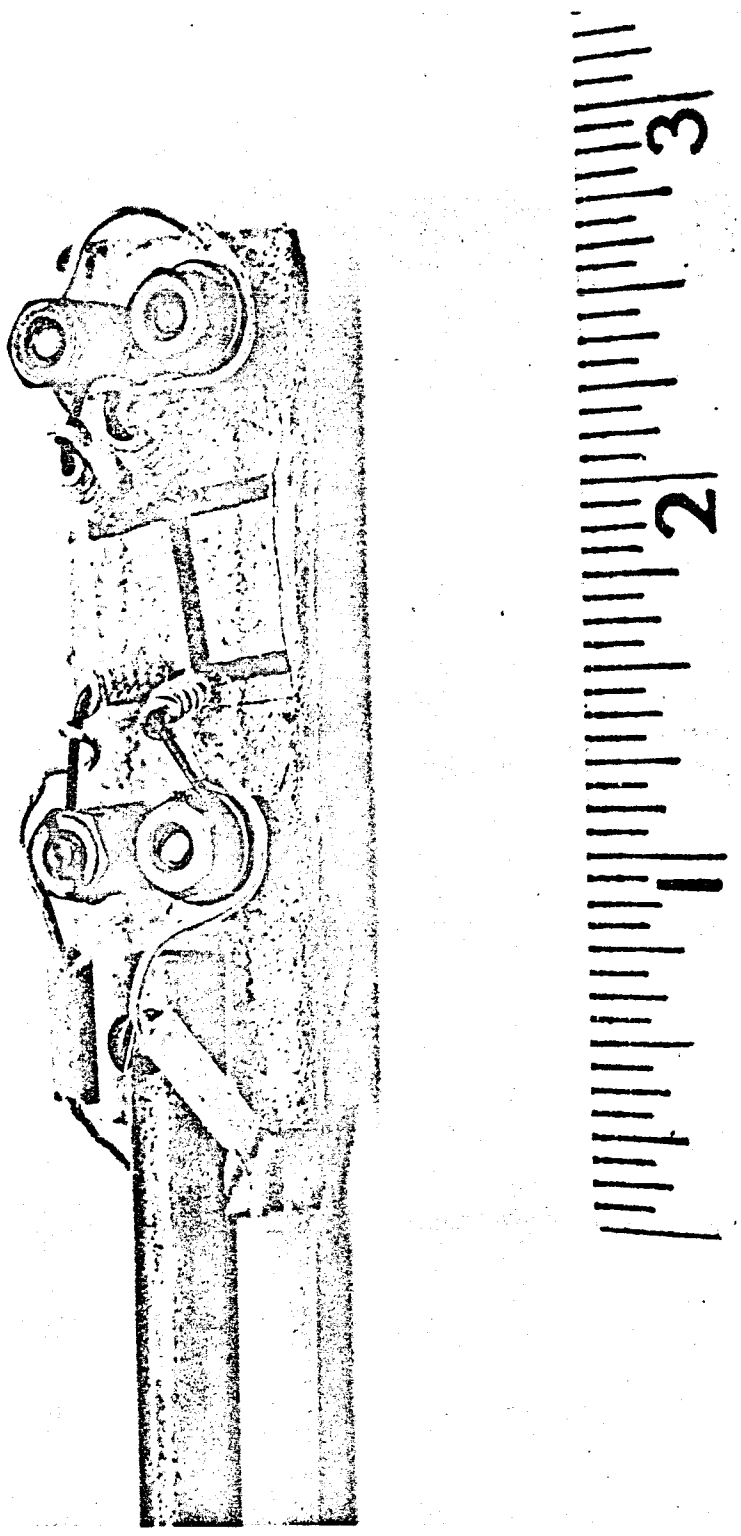

Fig. 35. Photograph of Four-Point Probe Used in Tube Oven

The film to be studied was placed on the asbestos block and held in place by the four probes which were gold or silver wire wound around tungsten wire cores.

In reference to Fig. 34, I_s was essentially a constant current determined by E_s/R_s since R_s was always much greater than R_x. The potential at node 1, determined by $I_s R_x$, is balanced by a similar circuit, determined by $I_R R_R$. As R_x changes with changing oxygen partial pressure, a potential difference occurs between nodes 1 and 5. Therefore, V is directly related to ΔR_x.

$$R_x = \frac{I_R R_R + V}{I_s} \tag{29}$$

$$\Delta R_x = \frac{V}{I_s} \tag{30}$$

3.2.1 Evaporated Gold

The most promising thin film material studied for its ability to sense oxygen partial pressure was vacuum evaporated gold. Film thickness in the range of 200 Å to 800 Å were studied in various environments. The geometry of the films is shown in Fig. 30. These structures were tested in environmental chambers previously discussed utilizing both the four point probe and the Wheatstone bridge measuring technique.

Figure 36 shows a plot of film resistance as a function of time for various environmental gases at 1 atmosphere pressure. This film was operated at a temperature of 173°C. These tests were made on the bridge with a temperature compensating film in use. As shown in Fig. 36, there is initially a slight increase in resistance followed by a large

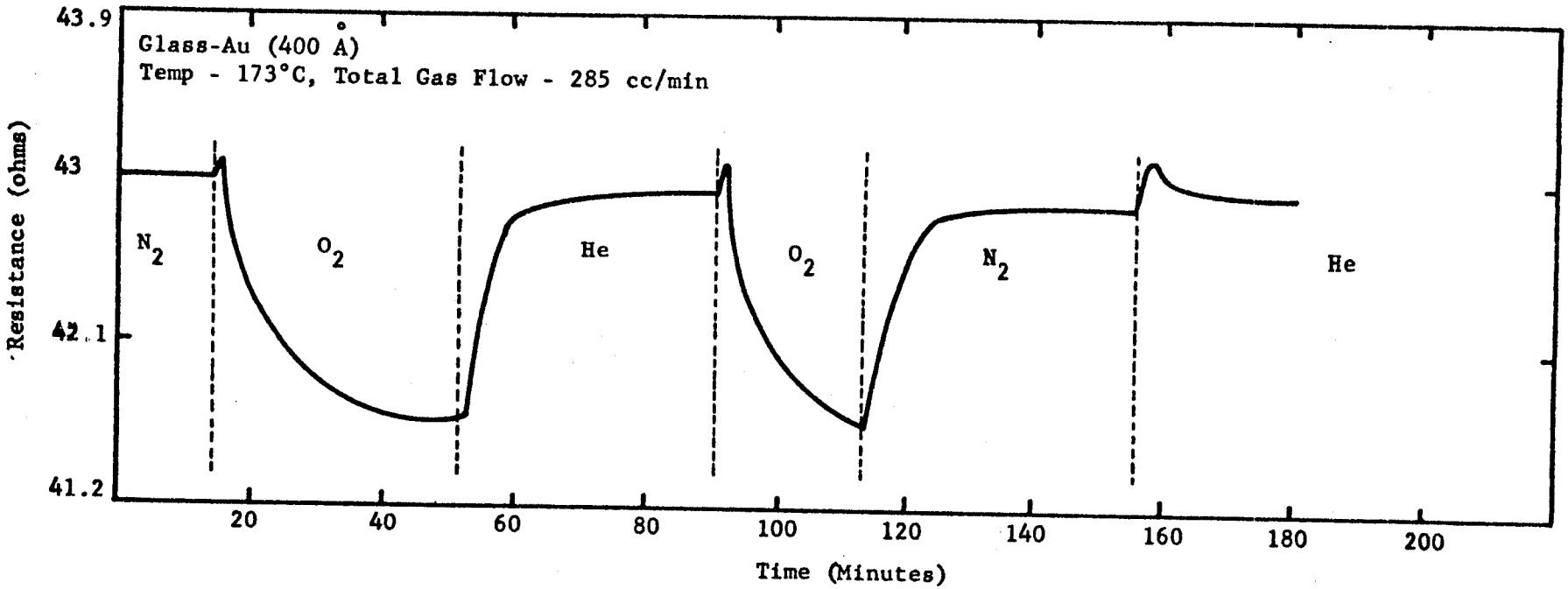

Fig. 36. Resistance vs Time in Various Environments

decrease after the film is exposed to oxygen following an inert environment.

In terms of the proposed scattering model, the initial increase could result from the formation of a monolayer of oxide which robs electrons from the conduction band thereby increasing resistance. Then as more oxide is formed, changes in the scattering process may become the dominate mechanism. The initial increase was seen in partial pressure measurements in which low oxygen pressure was used. In these experiments, the time in which the film resistance increased was much longer (> 10 minutes).

Figure 37 shows a semi-log plot of percent oxygen versus resistance of the film. Notice that the data points are best approximated by two straight lines.

In Fig. 38 is shown a time versus resistance plot for a gold sample at 155°C. The four-point probe method was used for this data. Note the long rise and fall times at this temperature. Figure 39 shows the same sample at 211°C. Notice that the rise times and fall times are more rapid, but the change in resistance from an inert atmosphere to oxygen is much smaller (0.90 ohms at 155°C and 0.40 at 211°C).

Figure 38 shows the drift that was encountered in the gold film with the four-point probe which used no temperature compensation film. It was found that the drift rate could be decreased considerably by annealing the film at 300° C before testing. However, the best method for drift and temperature compensation is a balancing masked film.

The data plotted in Figs. 38 and 39 is for a film which had a thickness of 400 Å. Data for other film thicknesses will be compared to the data for this film. The data plotted in Fig. 40 is for a film with a thickness of 800 Å. In this case, the change in resistance

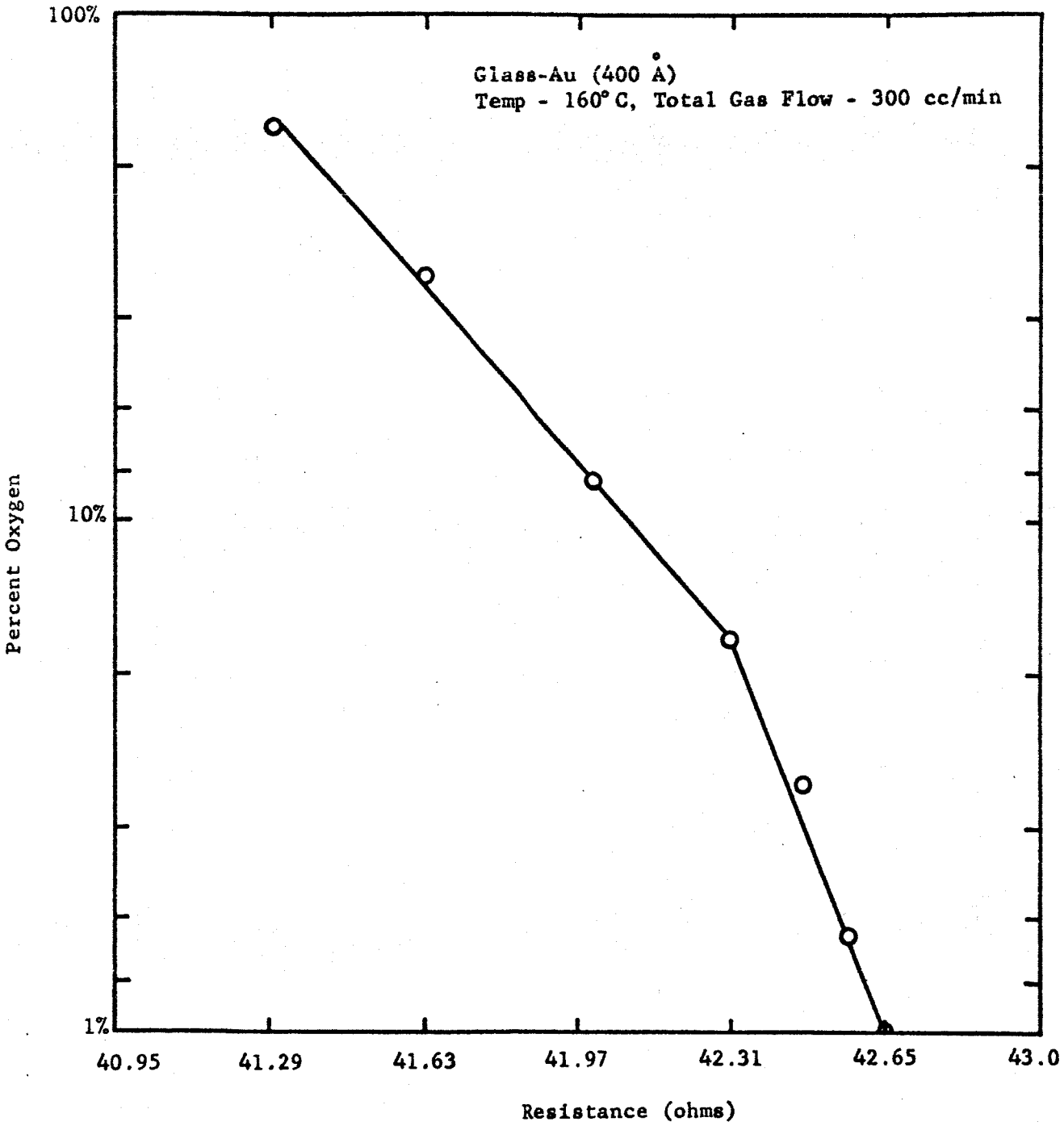

Fig. 37. Resistance Change vs Percent O_2

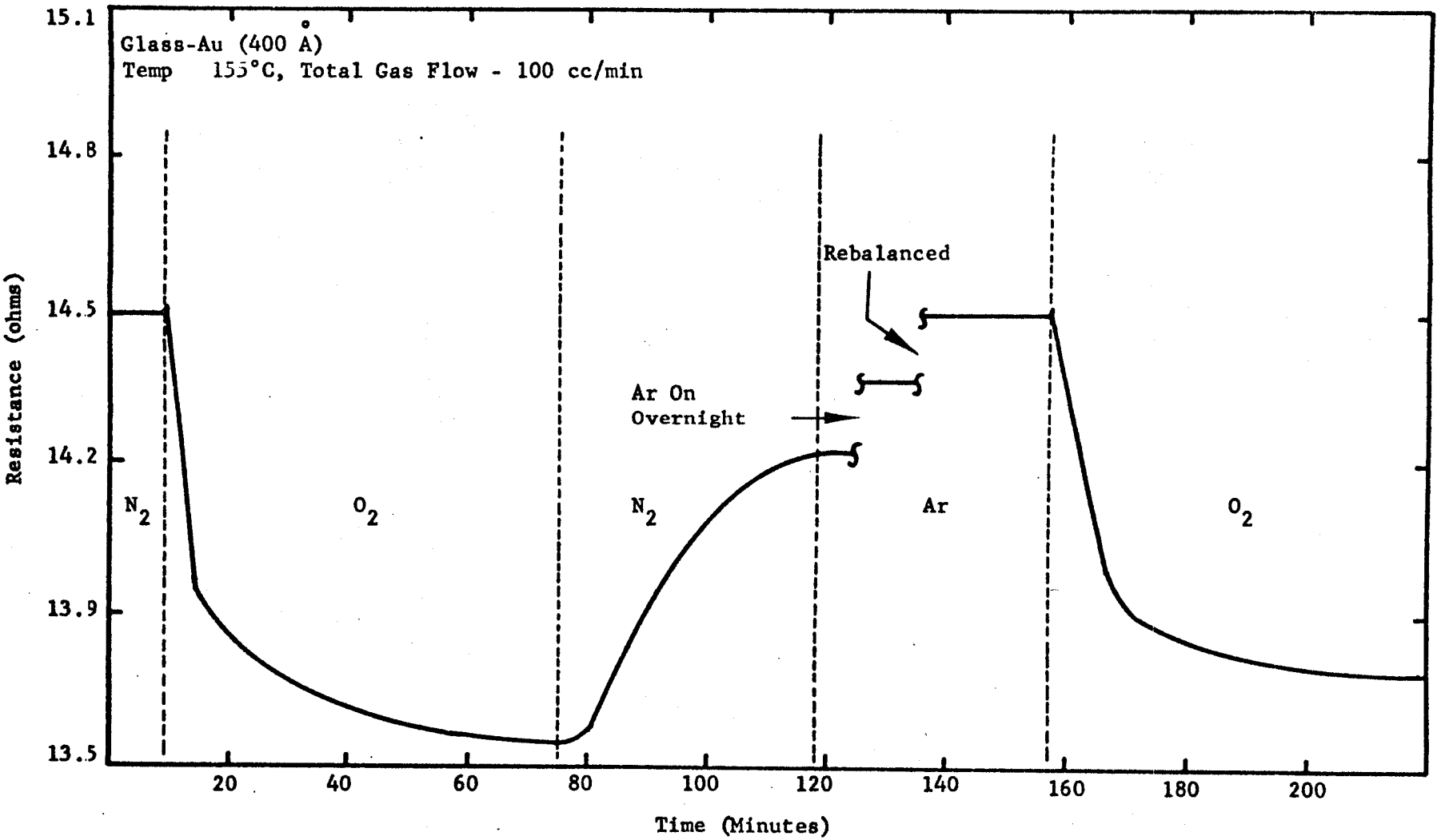

Fig. 38. Resistance vs Time in Various Environments

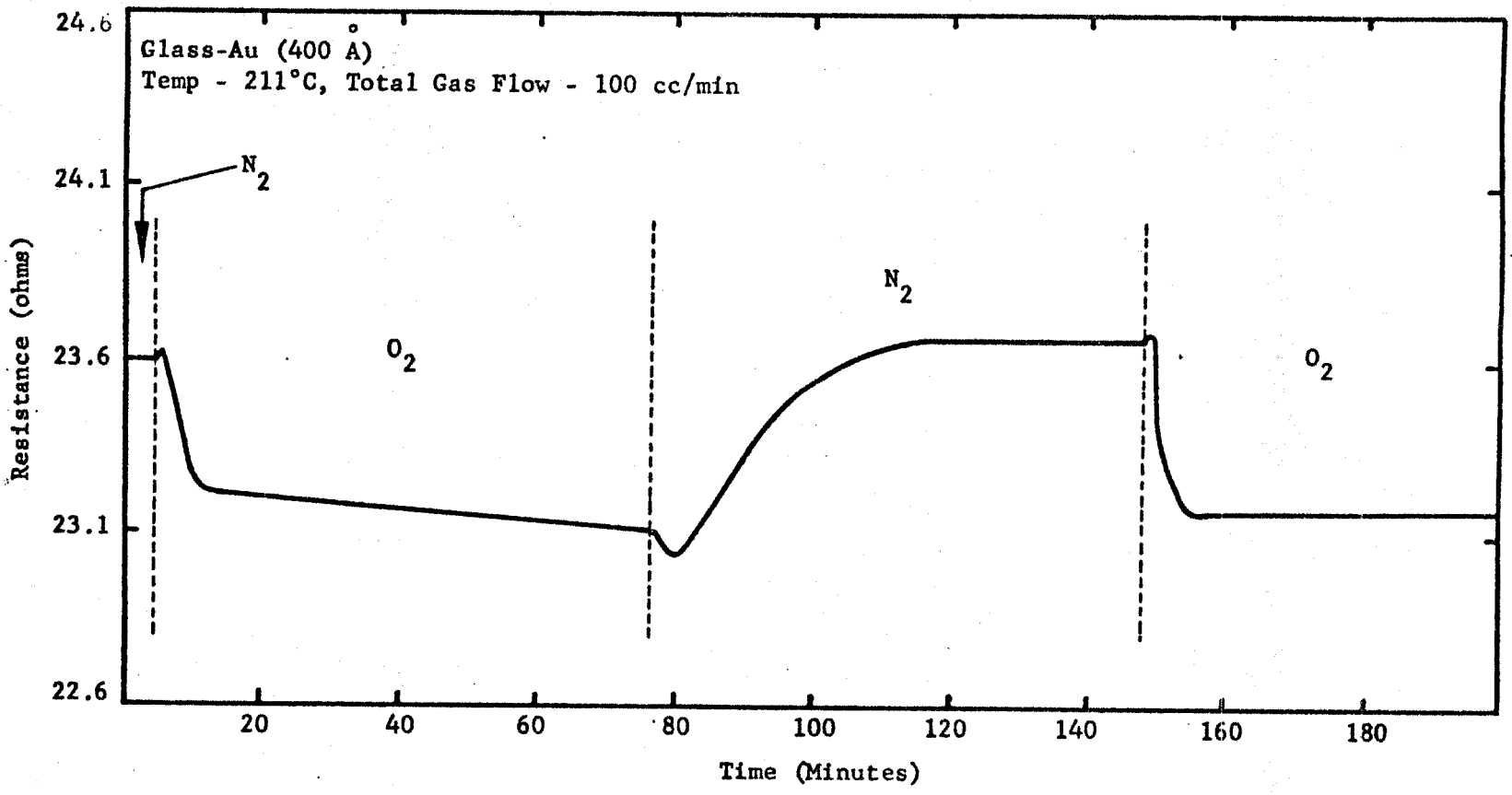

Fig. 39. Resistance vs Time in Various Environments

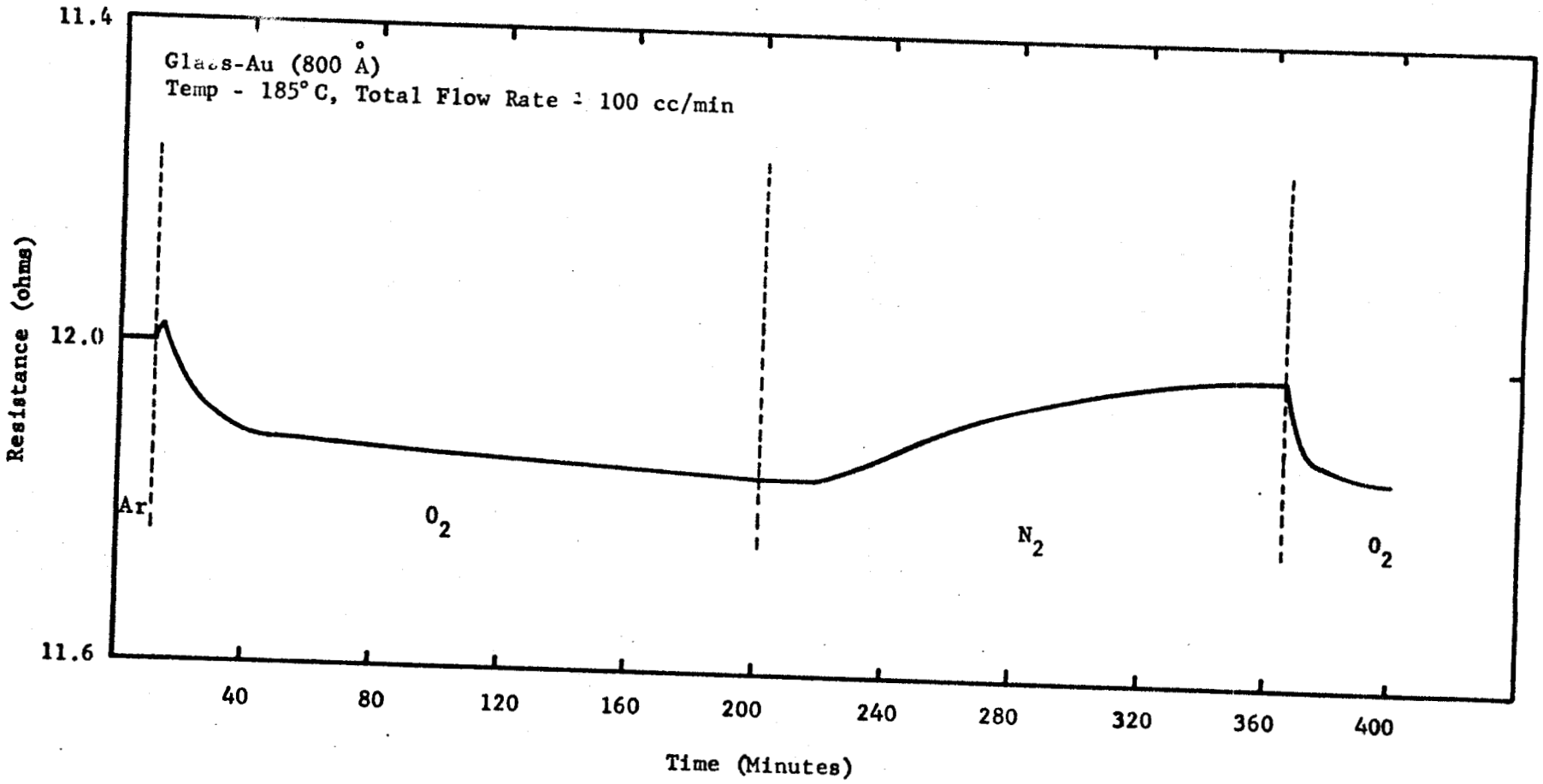

Fig. 40. Resistance vs Time in Various Environments

is much smaller than for the 400 Å films. Since the mean-free-path of conduction electrons in gold is about 400 Å, this was expected because the fraction of conduction electron specularly scattered at the surface of the film was less.

Although not shown in the figures, the resistance of gold film in water vapor and carbon dioxide was also checked. The films were found not to be sensitive to carbon dioxide and only slightly, if any more, sensitive to room air than to dry air.

Experiments have been made on gold film with soldered contacts. The experimental data was the same as that previously described for probes.

Figure 41 shows a plot of resistance change versus temperature for a particular gold film. Notice at lower temperatures, greater changes are exhibited. However, at lower than 150° C, the long time constant of change makes the total change difficult to detect.

Figure 42 shows a plot of rise time vs temperature. In order to produce a good oxygen sensor, a temperature will have to be selected that gives good resistance changes and fast rise times. Fast rise times usually mean fast fall times also.

3.2.2 Titanium, Zirconium, Hafnium

Zirconium and hafnium were found not to be sensistive to oxygen except for the formation of oxides at the temperature range investigated (room temperature to 300° C). The samples were manufactured in the geometry of Fig. 30 and tested in the test chamber described previously.

Oxides of zirconium and hafnium were also manufactured by placing a film of zirconium and hafnium in an oxygen environment at 800° C.

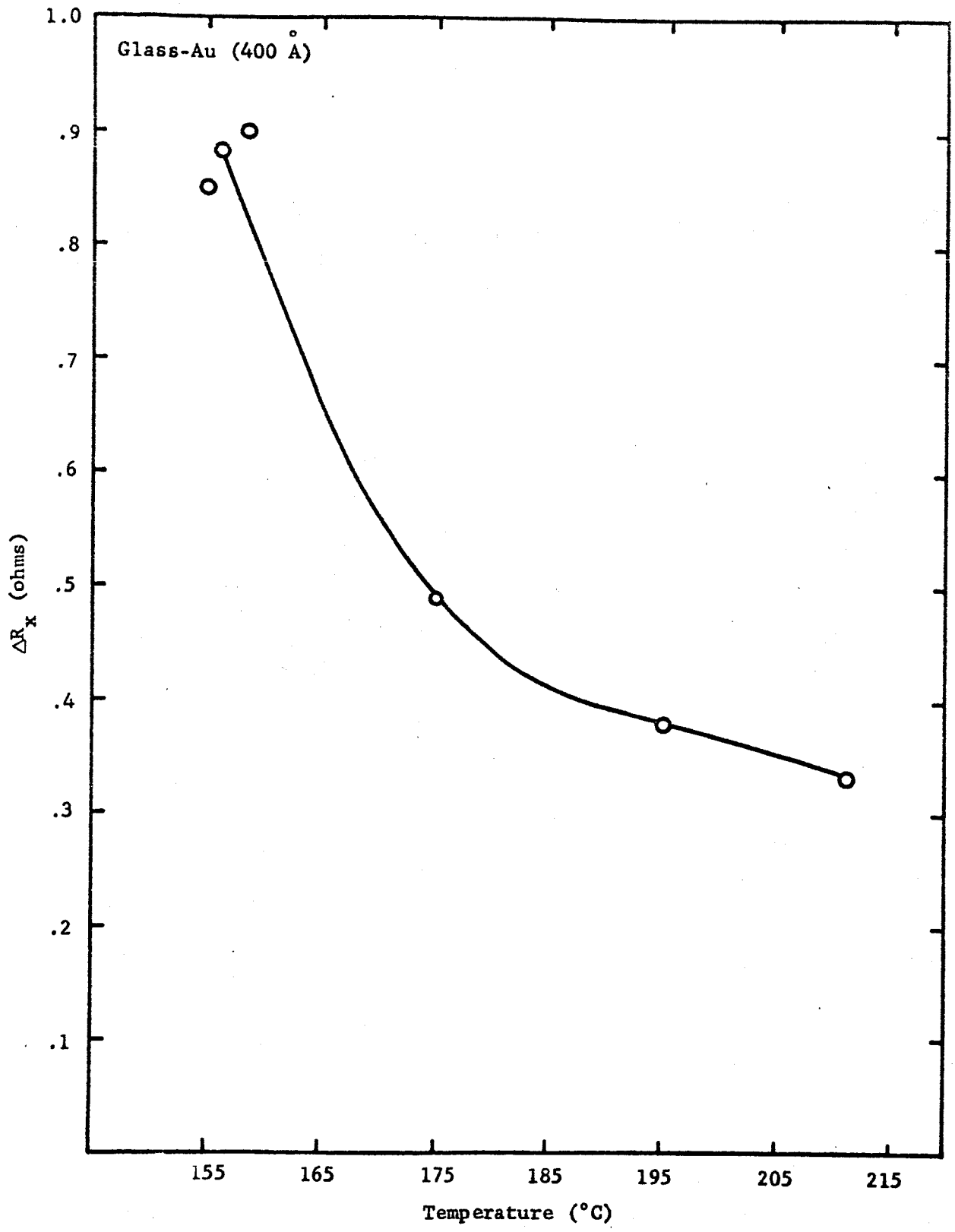

Fig. 41. Resistance Change on Change from an Inert Atmosphere to Oxygen vs Temperature

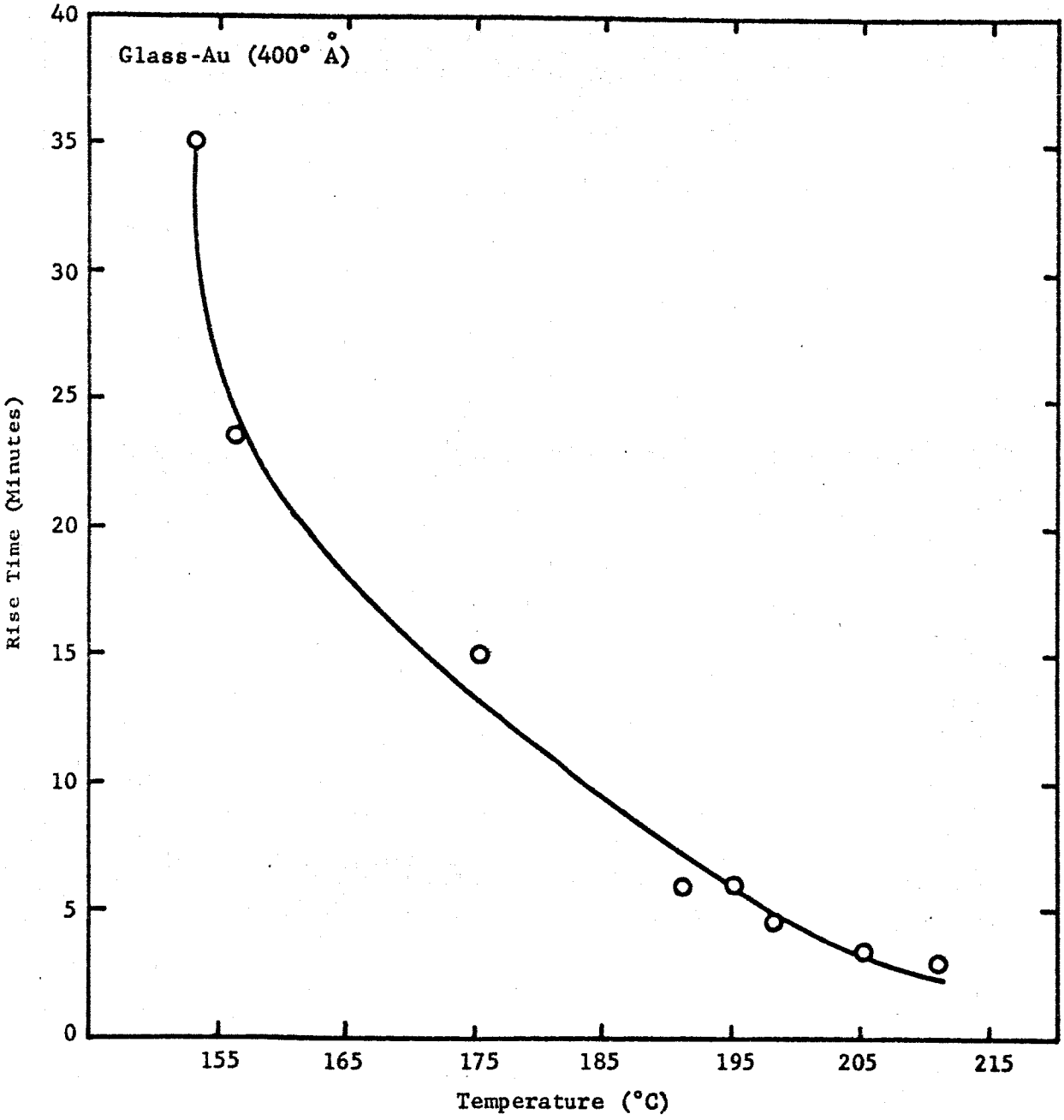

Fig. 42. Rise Time on Change from an Inert Enviroment to Oxygen vs Temperature

The electrical resistance of these oxides exhibited no dependence on oxygen pressure within the limits of the measuring apparatus (~ 0.1%).

Figure 43 shows the voltage unbalance of a Wheatstone bridge, with a hafnium sample as one leg, versus time in various environments. Notice that the electrical resistance of the film exhibits a dependence on the pressure of any gas. This effect was also seen in zirconium, but not investigated further since it was not oxygen related.

Only titanium was found to be oxygen sensitive. Figure 44 shows a plot of voltage from a Wheatstone bridge versus time in various environments for a titanium sample. Notice that the film is sensitive to both nitrogen and oxygen. This is not illogical since titanium is a very good "getter" of both oxygen and nitrogen. However, it was not possible to duplicate this data in the lab. The reason for this may have been that the low voltage due to the change in resistance of the film was overridden by external noise from the rest of the circuit.

Some samples of titanium made in the geometry of Fig. 30 showed reaction to oxygen, but it may have been the liquid bright gold and not the titanium whose resistance was changing.

3.2.3 Manganese, Silver, Nickel

Manganese, silver, and nickel were made in the geometry of Fig. 30 and tested in the Wheatstone bridge. The electrical resistance of these elements showed no dependence on oxygen pressure. Nickel oxide films were also manufactured but their resistance was too high to be tested accurately with the instruments available.

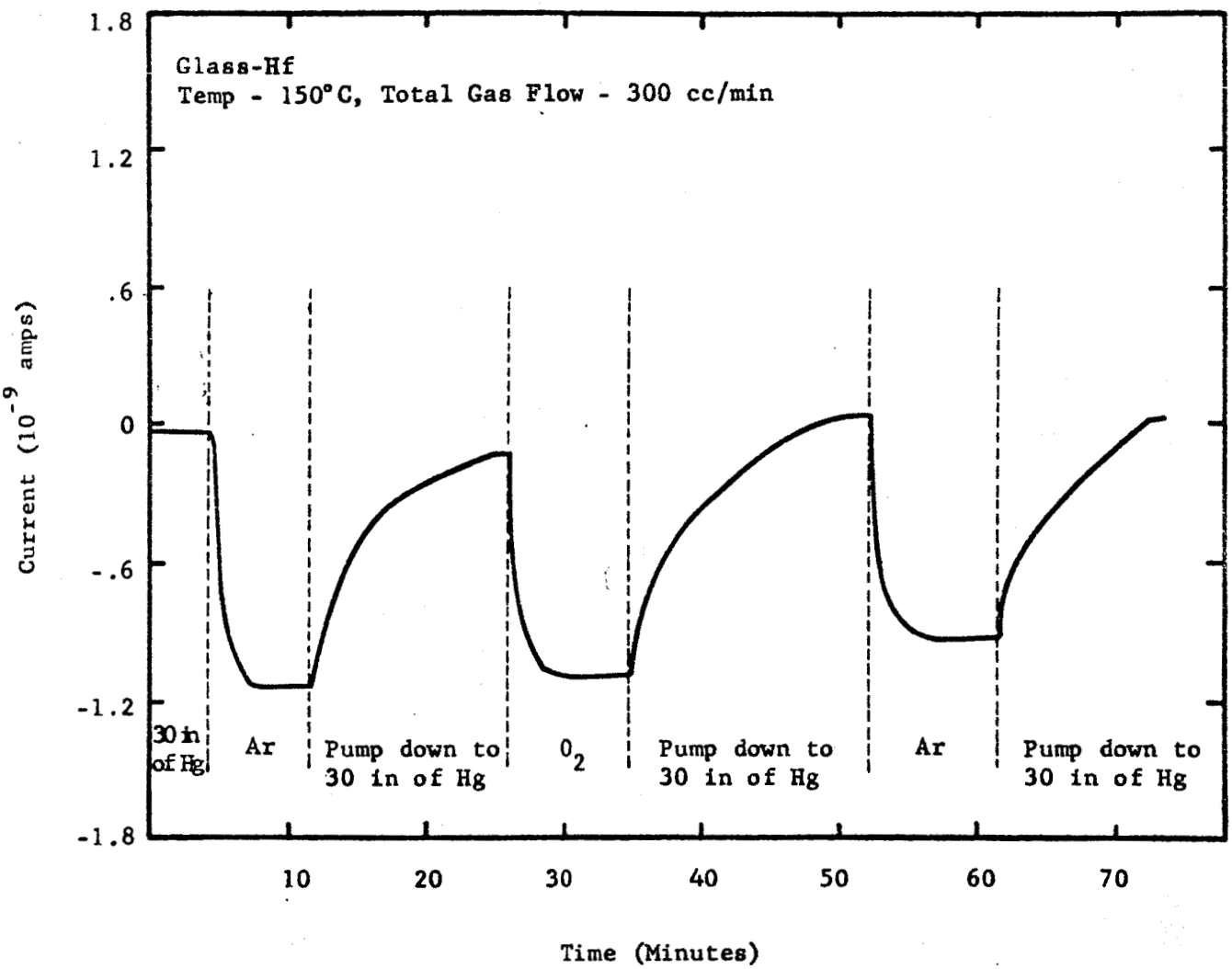

Fig. 43. Short-Circuit Current vs Time for Various Environments

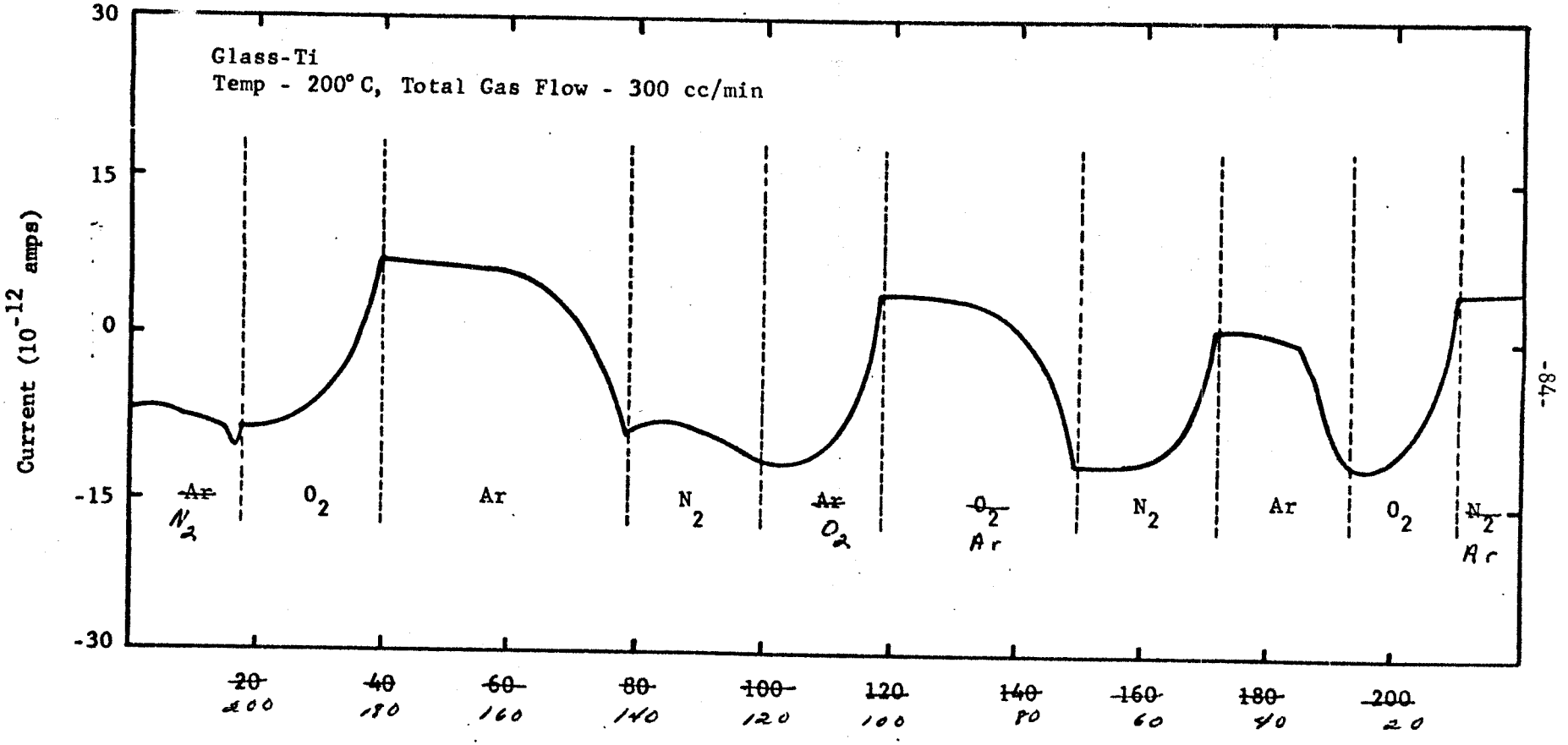

Fig. 44. Short-Circuit Current vs Time for Various Environments

3.2.4 Summary

The evaporated gold films are by far the most promising oxygen sensors of the conductance modulation type. Hafnium and zirconium may show resistance dependence on oxygen pressure, but only at extremely high temperatures (greater than 800°C). This reason alone may bar them from consideration. As previously noted, manganese, nickel and silver exhibited no dependence of resistance on oxygen pressure. The resistance of titanium may yet prove to be related to oxygen pressure in a feasible temperature range. However, the slight sensitivity shown so far may prove difficult to detect.

Gold oxygen sensors have proved to be dependable and rugged. They are easy to manufacture and easy to test. The effect of oxygen seems completely reversible so the lifetime should not be limited by consumption of an electrode as in the galvano-diffusion effect.

4. CONTROLLED OXIDATION

Another possible method of utilizing thin films as oxygen partial pressure sensors is the controlled oxidation of a conducting film. Consider a thin film of metal (a good conductor) which will oxidize in an oxygen environment to form an insulating metal oxide. Assuming that the film is thick enough so that bulk effects are the prominent factors, then

$$R(t) = \frac{\rho \ell}{WL(t)} \tag{31}$$

where R = resistance

ℓ = length

W = width

$L(t)$ = time dependent thickness

ρ = resistivity

If the metal oxide is a good insulator, the resistance is a function of the thickness as given by the above equation.

The parabolic growth rate is by far the most common growth law for metal oxides in an oxidizing environment,

$$L_{ox}(t) = Kt^{1/2} , \tag{32}$$

where $L_{ox}(t)$ is the time dependent oxide thickness, t is the time, and K is constant which is, among other things, a function of temperature and oxygen partial pressure. For the above growth law, the resistance of the film is

$$R = \frac{\rho \ell}{W(L(0) - Kt^{1/2})} \tag{33}$$

where L(0) is the metal film thickness at t = 0. The conductance G = 1/R is

$$G - G_o = -Kt^{1/2} , \tag{34}$$

where G_o is the conductance at t = 0.

As can be seen from the above equation, if one plots conductance as a function of time on log-log paper, a straight line will result with a slope of 1/2. If one knows from experiment or theory the dependence of K on oxygen partial pressure, then the oxygen partial pressure can be determined from a measure of the conductivity as a function of time.

A plot of log G vs log t will result in a straight line for the general case where the oxide growth rate is proportional to a power, n, of time, i.e.

$$L_{ox}(t) \propto t^n . \tag{35}$$

The slope in this case is n.

There are several disadvantages to this method. First of all one must find a material with the desired properties. This in itself is a major task. Aside from this problem, a considerable amount of electronics would be required to give a direct readout from such a sensor. Most oxidation processes in which the oxide is in direct contact with the oxidizing environment (no shielding as in the case of the galvano-diffusion structures) are extremely sensitive to water vapor and other impurities. Water vapor usually speeds up the process considerably.

It was decided that no specific experimental work would be performed on the controlled oxidation method. It was felt that the galvano-diffusion and conductance modulation methods showed much more promise.

5. CONCLUSIONS

Three thin-film techniques for sensing oxygen partial pressure have been studied: (1) galvano-diffusion, (2) conductance modulation, and (3) controlled oxidation. Of the three techniques, galvano-diffusion and conductance modulation received about equal efforts with minor emphasis on controlled oxidation. Based on the results of the study, it is concluded that the conductance modulation method is the better of the three techniques studied. In particular, the thin gold films show considerable promise.

In comparison with other techniques such as paramagnetic, galvanic cells, polarographs, UV spectrometers, mass spectrometers, chemical and activation analysis, thin film techniques are particularly attractive. Either the galvano-diffusion or conductance modulation technique when fabricated into a sensor will be small in size, light weight, and rugged. In addition power requirements are low. One major advantage that thin film sensors have over some of the more conventional instruments is that there is essentially no consumption of the oxygen and no reference oxygen supply is needed as is the case of galvanic cells. Direct readout with simple electronics is also a feature of thin film sensors.

The galvano-diffusion sensor has been shown to be operable as an oxygen partial pressure detector. The major advantages of this method over other methods studied are the relatively low temperature operation, wide pressure range, and the active nature of the phenomenon (no power required for electrical readout). There are several problems to be solved in applying this technique. First is the changing characteristics

with time. Since these changes result from the active nature of the processes involved, it is not possible to completely eliminate the changes. A second problem is the high inherent impedance of the devices. This results in low external current levels which are difficult to detect and which enhance electrical noise. The third and most difficult problem is not related to the phenomenon involved but rather to the state-of-the-art techniques in thin films. This is the problem of nonuniformity and inconsistency in film properties. Inconsistent dielectric films exhibit considerable variations in characteristics of sensors. Until better dielectric materials or better techniques are developed, it will be difficult to utilize the galvano-diffusion phenomenon as an oxygen partial pressure sensor.

The major disadvantages to the controlled oxidation technique are (1) indirect readout, (2) changing characteristics with time, and (3) short life for reasonable accuracy. Aside from the inherent disadvantages is the lack of any well-suited materials.

The only material which has been found suitable for utilization in the conductance modulation technique was gold. Based primarily on the theoretical study, other materials such as hafnium and zirconium oxides will require very high temperatures for operation ($\sim$ 1000°C) and will result in low sensitivities. On the other hand gold films can be operated at relatively low temperatures ($\sim$ 200°C) with reasonable sensitivities. In addition the gold films are relatively easy to fabricate using ordinary vacuum techniques. The major advantage of the conductivity modulation techniques over the other methods studied is the long life (no active processes involved) and reversibility. The major

problem is the relatively long time constants encountered when the environment is changed. Although the effect is temperature sensitive, bridging techniques can be used to compensate for these changes.

In conclusion the feasibility of utilizing thin film oxygen partial pressure sensors of the galvano-diffusion and conductance modulation types have been demonstrated. The use of gold films is concluded to be the most attractive sensor.

6. RECOMMENDATIONS

This study has been concerned primarily with determining the feasibility of using thin film devices as oxygen partial pressure sensors. A large number of materials have been evaluated as constituents in these thin film oxygen sensors. In order to determine the practical applicability of both types, galvano-diffusion and conductivity modulation, the next step is to fully investigate each of these with the most promising materials. The possibility of fabricating thin film nitrogen as well as other gas partial pressure sensors should also be considered. An experimental program is suggested in which (1) the galvano-diffusion effect studies are extended to structures using organic materials as dielectric (mylar for example), (2) gold and titanium conductivity modulated sensors are critically evaluated and (3) the feasibility of utilizing thin films in sensors of gases other than oxygen is investigated.

6.1 Conductivity Modulated Sensors

Sensors of the conductivity modulated type should be fabricated and evaluated. In particular the effects of film thickness, temperature, nitrogen, argon, helium, carbon-dioxide and water vapor should be determined and the long term stability investigated. It is expected that this phase of the program be a major part of the total program.

6.2 Galvano-Diffusion Sensors

Some organic materials such as mylar are very good electronic insulators and at the same time exhibit ionic conductivity. Since these

materials cannot be easily evaporated, thin sheets should be used with vacuum evaporated metal electrodes. Emphasis should be put on reducing the time of response and on improving reproducibility.

6.3 Partial Pressure Gas Sensors Other than Oxygen

The feasibility of sensing other gases by thin film techniques should be investigated. This should include N_2, Ar, He, CO_2 and H_2O. Particular attention should be given to the possibility of sensing nitrogen with titanium films. This phase of the total program should utilize as much information as possible from the other two phases.

REFERENCES

1. A. T. Fromhold, Jr., J. Phys. Chem. Solids 24, 1963, pp. 1081-1092.

2. A. T. Fromhold, Jr., J. Phys. Chem. Solids 25, 1964, pp. 1129-1137.

3. S. Dushman, Scientific Foundations of Vacuum Technology 2nd Edition, New York, John Wiley and Sons, Inc., 1962, Chap. 6.

4. I. Langmuir, J. Am. Chem. Soc. 40, 1918, p. 1361.

5. S. Brunauer, P. H. Emmett and E. Teller, J. Am. Chem. Soc. 60, 1938, p. 309.

6. L. Holland, Vacuum Deposition of Thin Films, New York, John Wiley and Sons, Inc., 1960, Chap. 4, pp. 110-114.

7. C. van Hoerden and P. Zwietering, Koninkl. Ned. Akad. Wetenschap. Proc. B60, 1957, p. 160.

8. R. Suhrmann, G. Wedler and D. Schliephake, Z. Physik. Chem. (Frankfurt) 12, 1957, p. 128.

9. E. H. Sondheimer, Advances in Physics (supplement of Phil. Mag.) 1, 1952, p. 1.

10. H. A. Laitinen and M. S. Chuo, J. Electrochem. Soc. 108, 1961, pp. 726-731.

11. M. L. Gimpl, A. D. McMorter and N. Fuschillo, JAP 35, 1964, pp. 3572-3575.

12. G. Ehrlich, J. Chem. Phys. 35, 1961, pp. 2165-2167.

13. H. Saltsburg and P. P. Snowden, Surface Science 2, 1964, pp. 288-297.

14. J. Rudolph, Z. Naturforsch. 14a, 1959, p. 727.

15. D. S. Tannhauer, Solid State Communications 1, 1963, pp. 223-225.

16. A. von Hippel, S. Kalnajs and W. B. Westphal, J. Phys. Chem. Solids 23, 1962, p. 779.

17. P. Kofstad and D. J. Ruzicka, J. Electrochem. Soc. 110, 1963, pp. 181-184.

18. R. W. Vest and N. M. Tallan, J. Am. Ceramic Soc. 48, 1965, pp. 472-475.

REFERENCES (continued)

19. R. W. Vest, N. M. Tallan and W. C. Tripp, J. Am. Ceram. Soc. 47, 1964, pp. 635-640.

20. T. Smith, J. Electrochem. Soc. 111, 1964, pp. 1020-1027.

21. T. Smith, J. Electrochem. Soc. 111, 1964, pp. 1027-1031.